Energy Advances

ROYAL SOCIETY OF CHEMISTRY

PAPER

View Article Online
View Journal | View Issue

Cite this: *Energy Adv.*, 2026, 5, 550

Life cycle assessment of grid-scale battery storage: evaluating the environmental competitiveness of sodium-ion systems

Friedrich B. Jasper, *[ab] Yuhuan Zhou,[a] Hüseyin Ersoy,[a] Manuel J. Baumann, [a] Jens Peters, [c] Dirk Holger Neuhaus[bd] and Marcel Weil *[ae]

Received 21st November 2025,
Accepted 26th February 2026

DOI: 10.1039/d5ya00341e

rsc.li/energy-advances

The large-scale deployment of stationary battery storage is critical for enabling renewable energy integration, yet life cycle assessments (LCAs) of these systems often overlook the contributions of balance-of-system (BOS) components. This study establishes a life cycle inventory (LCI) model for two container storage systems (CSSs), a liquid-cooled and an air-cooled system. Consequently, a full LCA is carried out with four different cell types, focusing on sodium-ion batteries (SIBs). The resource and environmental impacts of all BOS subsystems, including containers, thermal management systems (TMSs), power converters, control systems and auxiliary components, are investigated in detail. The results show that BOS components contribute between 32 and 58% of impacts in global warming potential (GWP) and 63–88% in resource use, minerals and metals, emphasizing their significant role in the sustainability of grid-scale storage. Due to its high demand for copper and steel, a transformer is particularly important in this regard. However, the environmental impact attributable to its production can be reduced through correct dimensioning and adequate recycling. It is further shown that SIBs are competitive with lithium-ion batteries in CSSs with regard to environmental impacts, despite their lower energy densities. By shedding light on previously underexplored system elements, this work provides a robust foundation for more comprehensive LCAs of containerized battery storage solutions and enables more informed design, scaling, and policy decisions for future energy systems.

1. Introduction

1.1. Background

With the global energy transition, the share of electricity generated from renewable sources is consistently increasing. Solar energy and wind energy, however, depend heavily on meteorological conditions, leading to significant intermittency and volatility. This intermittency means that the supply of electricity can no longer be synchronized with the demand, so energy has to be stored temporarily. Energy storage systems (ESSs) offer a viable solution to this problem. ESSs can balance this discrepancy by storing excess energy during peak production periods and releasing it when production is low or demand is high.[1] Battery energy storage systems (BESSs) in particular are widespread and recognized for their rapid response capability, continuous power supply capability, cost efficiency and geographical independence.[2,3] They offer broad application prospects in the grid system due to high possible capacity, high reliability, high flexibility, and strong environmental adaptability.[4] These advantages make BESSs particularly suitable for stabilizing the energy grid, which is a significant challenge for systems with higher shares of renewable energy sources, and has resulted in significant global growth opportunities.[5] At the grid level, BESSs are often container storage systems (CSSs) allowing mobility and scalability. The global containerized BESS market was valued at 16 billion US dollars in 2024 and is expected to reach 44 billion US dollars by 2031, with a compound annual growth rate of 15.2% during the forecast period from 2025 to 2031.[6] Precedence Research projects an even higher annual growth rate of 27% for the full BESS market between 2025 and 2034.[7]

The growing importance and commercial success of CSSs suggest that they will play a key role in future energy infrastructure. Therefore, comprehending containerized ESSs and all their implications is essential for the shift to clean energy systems. Although BESSs can contribute significantly to the energy transition and therefore reduce the environmental

[a] *Institute for Technology Assessment and Systems Analysis (ITAS), KIT, Karlsruhe, Germany. E-mail: friedrich.jasper@kit.edu, marcel.weil@kit.edu*
[b] *Department of Sustainable Systems Engineering (INATECH), University Freiburg, Germany*
[c] *Department of Economics, University of Alcalá, Alcalá de Henares, Spain*
[d] *Fraunhofer Institute for Solar Energy Systems (ISE), Freiburg, Germany*
[e] *Helmholtz-Institute for Electrochemical Energy Storage (HIU), KIT, Ulm, Germany*

impact per kWh of electricity consumed, the systems come with their own environmental impact. A comprehensive assessment can identify key contributors, enabling the optimization of system design to minimize these effects. Moreover, such analyses can improve the environmental performance of energy systems overall by providing an in-depth understanding of storage technologies, which is crucial for future systems.

Life cycle assessment (LCA) is a widely used tool for identifying environmental hotspots and comparing alternative systems.[8,9] A large number of studies have assessed the environmental impact of batteries.[10] While many of these studies do not focus on a specific application, most of the assessed applications are mobile, such as electric vehicles or consumer electronics, rather than stationary.[11,12] In the following literature review an overview of all LCAs of grid-scale BESSs is shown.

1.2. Literature review

As a part of this study, a literature review was conducted on the LCA of all grid-scale BESSs. Google Scholar and Science Direct were used, with the keywords ''life cycle assessment'', ''LCA'' and ''environmental impacts'' combined with ''battery energy storage system'', ''energy storage system'', ''batteries in stationary application'', ''container storage system'' and ''CSS''.

Table 1 shows studies identified which addressed the environmental impact of grid-scale BESSs from 2015 to 2025. For each study, the year of publication, functional unit (FU), system boundaries, the considered cell types and their life cycle inventory (LCI) data source, the LCI data source of the battery management system (BMS) and all other balance-of-system (BOS) components considered are listed. Even though there is no standard definition of the BOS components of such systems, these usually further include module housing, a power conversion system (PCS), a thermal management system (TMS), a container, a controller and others such as a fire protection system. All necessary components for CSSs are explained in detail in Section 2.2.

Notably, despite the importance of CSSs for renewable energy transition, only 16 studies were identified that quantify the environmental impacts of such systems. While all of the studies consider the production and use phases, eleven also assess end-of-life (EOL) of the system. However, consideration of BOS components that exceed the module level is limited to five studies. These include studies of Abdon *et al.* (2017), Raugei *et al.* (2020) and Da Silva Lima *et al.* (2021), which consider only a few BOS components, such as inverters and cables in their assessments.[13–15]

Only the two recent studies by Komesse *et al.* (2024) and Wickerts *et al.* (2023) incorporate additional BOS components.[16,17] Although Komesse *et al.* (2024) additionally includes the container and a ventilation system, several key elements remain excluded from the system boundaries, including a fire suppression system, advanced cooling systems (beyond simple rack fans), transformers, certain electronic components (such as screens and wiring), and a concrete foundation.[16] Furthermore, several of the component models used in the study rely on outdated data. For example, the BMS is based on Bauer (2010).[18] The battery cells are modeled based on Majeau-Bettez *et al.* (2011), which is cited as providing the only available data on cylindrical cells.[19] Additionally, the model is adapted to different cell types by interchanging them based on the overall energy capacity, while differences regarding energy density are disregarded. Another limitation of the study by Komesse *et al.* (2024) lies in the system scale: the modeled container system has a storage capacity of only 192 kWh, whereas current commercial systems typically range between 1 and several MWh per 20-foot container.[16] This discrepancy is primarily due to the limited data availability on CSSs, as well as the study's reliance on the one system design described by Schimpe *et al.* (2018).[20]

The study by Wickerts *et al.* (2023) has been identified as the one which includes the most BOS components while conducting an LCA of a grid-scale BESS.[17] Although the focus of the study lies on lithium-sulfur batteries, the most prominent BOS components are considered based on scientific literature and ecoinvent. However, due to the focus of the study, modelling is limited in terms of the level of detail. Often, a component identified in the literature was modelled using a scaling factor based on kg kWh^{-1}, combined with a dataset from ecoinvent. Consequently, the cooling system is represented only by fans in the modules, and the fire suppression system by a tank full of CO_2 rather than by entire systems. Additionally, neither a controller for the entire system nor a transformer was taken into account. These limitations found in the literature review underline the need for updated, comprehensive LCAs that reflect modern designs and operational scales in CSSs.

1.3. Aim

The conducted literature review shows a significant research gap in the assessment of the environmental impacts of CSSs, especially with regard to the inclusion of BOS components. To address this gap, this study conducts an LCA of two CSSs with different system layouts: one with an air-cooling system and one with a liquid-cooling system. To the best of the authors' knowledge, this is the first work to include all the necessary BOS components of a CSS. The two systems are assessed with three emerging sodium-ion battery (SIB) chemistries and the dominant lithium-ion battery (LIB) technology, giving in total eight different system configurations. The study aims to evaluate the environmental impact of CSS peripheral components and enable future research to examine the environmental impacts of batteries in stationary grid-scale applications by establishing the life cycle inventory (LCI) of a containerized, grid-scale BESS.

2. Methodology

2.1. Assessment framework

LCA is the central tool for assessing the environmental impact of products and processes. It can consider all three phases of the product's life cycle: the production phase, including the extraction of raw materials, the use phase, and the EOL phase

Table 1 Literature review of studies conducting an LCA of grid-scale BESSs from 2015–2025

Study	Year	Functional unit	System boundaries	LIB cells considered	BMS	Other BOS components
Stanchev and Hinov[21]	2025	1 MWh energy delivered	Production, use phase and EOL	Not apparent	Not apparent	Not apparent
Komesse *et al.*[16]	2024	Daily energy restitution	Production, use phase and EOL	LFP and NMC, both based on Majeau-Bettez *et al.*[19]	Bauer[18]	Inverters, containers, and ventilation systems (all based on ecoinvent)
Li *et al.*[22]	2024	1 MWh energy delivered	Production and use phase	LFP and VRFB based on primary data for cells	Han *et al.*[23]	Not considered
Wickerts *et al.*[17]	2023	1 MWh energy delivered	Production, use phase and EOL	Li–S based on Deng *et al.*[24] and other literature	Ellingsen *et al.*[25]	Inverters, containers, concrete, fire suppression, and ventilation systems (mainly based on ecoinvent)
Han *et al.*[23]	2023	1 MWh energy stored	Production, use phase and EOL	LFP, NMC, and VRFB based on primary data	Primary data	Not considered
Yudhistira *et al.*[26]	2022	1 kWh energy delivered	Production, use phase and EOL	LFP, NCA, and NMC based on Peters and Weil[27] and PbA based on Spanos *et al.*[28]	Ellingsen *et al.*[25]	Not considered, apart from module housing
Carvalho *et al.*[29]	2021	1 kWh energy delivered	Production, use phase and EOL	LFP, NMC 532 and NMC 622 based on primary data, Majeau-Bettez *et al.*[19] and Ellingsen *et al.*[25]	Ellingsen *et al.*[25]	Module housing and module cooling based on Ellingsen *et al.*[25]
Da Silva Lima *et al.*[14]	2021	1 MWh energy delivered	Production, use phase and EOL	NMC based on Majeau-Bettez *et al.*[19] and VRFB based on primary data and Weber *et al.*[30]	Weber *et al.*[30]	Tray housing, busbars, rack housing, fans, cables, and inverters
Raugei *et al.*[13]	2020	1 kWh energy delivered	Production and use phase	LMO based on ecoinvent, and in turn based on Notter *et al.*[31]	Notter *et al.*[31]	Structural elements and electrical components based on Leccisi *et al.*,[32] assessed in PV systems
Jones *et al.*[33]	2020	1 MWh energy delivered	Production, use phase and EOL	LFP based on Majeau-Bettez[19]	Not considered	Transformers, switchgears, and inverters
Vandepaer *et al.*[34]	2019	1 MWh energy delivered	Production, use phase and EOL	LFP based on primary data of undisclosed battery manufacturer collected for a previous study[35] and adjusted with literature[27,36]	Ellingsen *et al.*[25]	Module cooling based on Ellingsen *et al.*[25]
Ryan *et al.*[37]	2018	1 MW-yr of frequency regulation capacity	Production, use phase and EOL	LMO, LFP, NMC, and NCA based on BatPac	GREET[38]	Not considered, apart from module housing
Peters and Weil[39]	2017	1 kWh storage capacity	Production and use phase	LFP and LFP-LTO based on various sources[18,27,40]	Technical data sheets	Not considered, apart from rack and module housing
Abdon *et al.*[15]	2017	1 kWh energy delivered	Production, use phase and EOL	LTO and NCA based on ref. 41	Not apparent	Inverters and thermal management
Baumann *et al.*[42]	2017	1 kWh energy delivered	Production and use phase	LFP and NMC, among others, based on various sources[18,25,40,43]	Not considered	Not considered
Hiremath *et al.*[44]	2015	1 MWh energy delivered	Production and use phase	LFP, NMC and LMO based on ref. 19	Not apparent, presumably based on ref. 19	Not considered

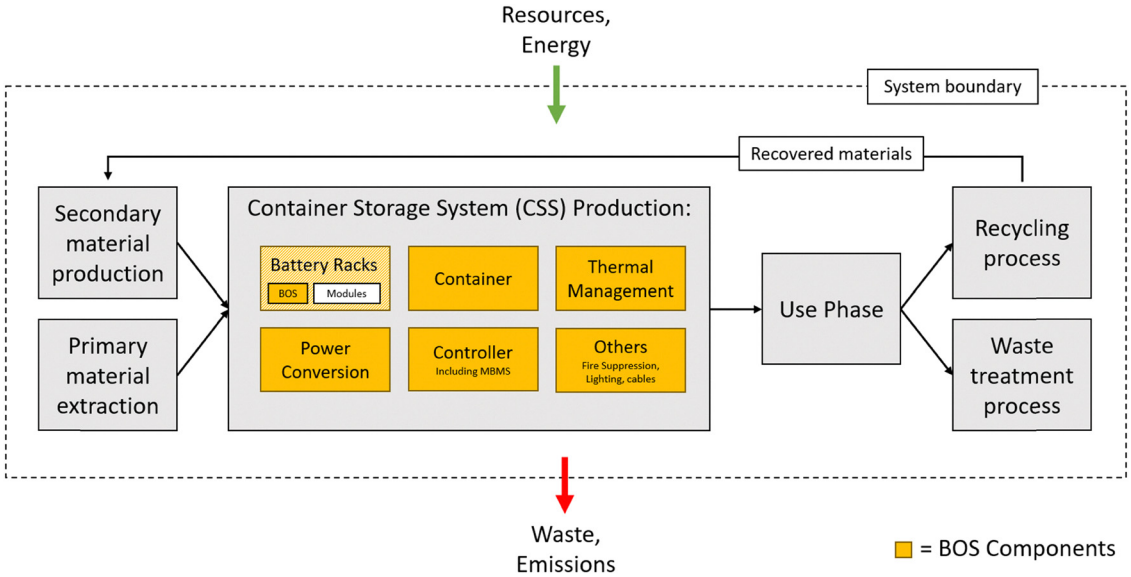

Fig. 1 System boundaries of the conducted LCA. Balance-of-system (BOS) components are highlighted as they are the focus of the study. The racks and module housing are also considered BOS components, but not the battery cells.

including recycling and/or final disposal. The methodology of LCAs is standardized by the International Organization for Standardization (ISO) in its guidelines 14040 and 14044.[8,9] These guidelines divide LCAs into four stages: (1) goal and scope definition, (2) life cycle inventory (LCI) analysis, (3) life cycle impact assessment (LCIA), and (4) interpretation of the results.

In line with these standards, the goal of this study is to assess the environmental impact of two CSSs, including all BOS components, and three SIBs, as well as one LIB as reference. The study assesses one CSS with an air-cooling system and one with a liquid-cooling system. Both system designs are equipped with either SIB or LIB cells. For the former, three different battery types are considered: based on (i) Prussian blue analogues (PBAs), (ii) a polyanionic material, and (iii) a layered metal oxide as the cathode active materials (CAMs), all paired with hard carbon on the anode side. The LIB, serving as a benchmark, relies on lithium iron phosphate (LFP) as the CAM paired with graphite on the anode side. The LFP cell technology is currently most common in stationary battery systems.[45] The study focuses specifically on the impact stemming from the peripheral components. The scope of this work includes all three phases of the life cycle, with the system boundaries set from cradle to grave, as shown in Fig. 1. The FU of the conducted LCA is 1 kWh of energy delivered, which best represents the main function of a CSS. It also takes into account round-trip efficiency and cycle life time and allows a comparison to be made with non-electrochemical storage systems. However, the production phase as well as the EOL phase are described per kWh energy capacity as this is a commonly used unit to compare different systems when no use phase is considered.

The LCI of the two CSSs was compiled using a variety of primary and secondary sources including scientific studies, academic databases, product data sheets, technical manuals and direct contact with manufacturers. A total of more than 30 sources were used, about half of which are scientific studies published in relevant journals, while the remaining are publicly available data sources from manufacturers. These sources show a wide variety of configurations and considerations related to BOS components. Unlike the studies presented in Table 1, these sources do not necessarily investigate the environmental impacts of CSSs, but instead present data or details on BOS components of CSSs. For instance, the study by Komesse *et al.* (2024) is not considered as it does not present new data on a CSS; instead, the underlying study by Schimpe *et al.* (2018) is included.[16,20] A detailed overview of the data presented in the sources can be found in the SI. While the presented systems vary in size from 200 kWh to around 4 MWh, it should be noted that all function with LIBs based on either the LFP or NMC cell type. Additionally, the fairly equal distribution of liquid- and air-cooling thermal management across the sources shows that both types of systems are relevant in the market. This is one reason why this study models both types of systems. The two most detailed data sources, from the manufacturers Power Sonic (air-cooled) and Symtech Solar (liquid-cooled), form the basis of the two CSS models presented in this study.[46,47] Data collection was supplemented by a field visit to a 4 MW solar power station in Germany, where battery energy storage containers function as a buffer, storing electricity when it is produced in excess and feeding it into the grid during periods of high demand. A detailed description of the LCI modeling and data sources for the individual components can be found in Section 2.3 and the SI.

For the LCIA, openLCA 2.5 software combined with the ecoinvent 3.11 database and the Environmental Footprint (EF) 3.1 method was used. This method is recommended by the European Commission and includes 16 impact categories.[48]

Section 3 shows the results in the categories climate change (global warming potential – GWP) and resource use, minerals and metals. GWP is the most widely discussed impact category and is mandatory within the scope of the EU's Battery Regulation and Product Environmental Footprint, making a closer look at the category necessary.[48,49] Mineral resource use is of particular interest with regard to the comparison between SIBs and LIBs, as SIBs are based on more abundant materials. However, as all impact categories may be of interest, the cradle-to-gate results for all impact categories of the LCIA method EF 3.1 are given in the SI. Additionally, this work provides the full LCI for both systems, enabling reproducibility and the adoption of a different perspective.

2.2. General CSS description

The structure and design of a CSS generally depend on various factors, including the intended application, operating environment, energy requirements, capacity, and size. This results in significant design variations across manufacturers.[50,51] A review of the data sources revealed that six key components are essential for a CSS: the battery racks, a container, a TMS, a PCS, a controller and the auxiliary system.

Fig. 2 shows a schematic representation of a CSS. The composition of the overall system is shown on the top level while the additional components of the battery racks, modules and cells are shown on subsequent levels.

2.2.1. Battery racks. Battery racks, meaning the collective assembly of all racks, form the core of the CSS. They encompass the battery modules, steel racks, high-voltage (HV) control boxes, the two lower levels of a three-tier BMS, and the associated cabling and auxiliary components. Each battery module, serving as the fundamental storage unit, consists of multiple battery cells connected in series. These cells are integrated with a battery module unit (BMU), a cooling duct equipped with fans, busbars, insulators, and a robust steel housing that provides structural integrity and protection.

Central to the proper functioning of the battery racks is the BMS, designed to maintain safe and efficient battery operation. Its key functions include thermal regulation, enforcement of current and voltage safety limits, fault detection and shutdown, and continuous estimation of both the state of charge (SOC) and state of health (SOH).[53] To perform these functions effectively, modern CSS configurations typically employ a hierarchical, three-level BMS architecture, facilitating communication and control from individual cells to the entire system.

At the lowest level, the BMU—embedded within each battery module—monitors the voltage and temperature of individual cells, performs active balancing to maintain uniform performance, and transmits data to the secondary BMS (SBMS).[54] The SBMS, located in the HV control box and representing the intermediate layer, consolidates data from all BMUs within a rack. It also oversees rack-level electrical protection by measuring voltage and current, controlling DC contactors, and ensuring isolation in the event of faults. At the highest level, the master BMS (MBMS) integrates information from all SBMS units across the system. It coordinates global safety functions, optimizes system performance, and issues operational commands to the lower BMS layers.[55] This hierarchical structure ensures robust monitoring, fault tolerance, and coordinated control throughout all battery racks of the CSS.

2.2.2. Container and thermal management system (TMS). The container, which houses the entire system, is typically based on a 20- or 40-foot ISO standard shipping container. Its interior walls are lined with flame-retardant materials such as rock wool to provide fire protection, thermal insulation, and noise reduction.[56] To further maintain safe operating conditions and reduce fire risk, as well as lower degradation rates,

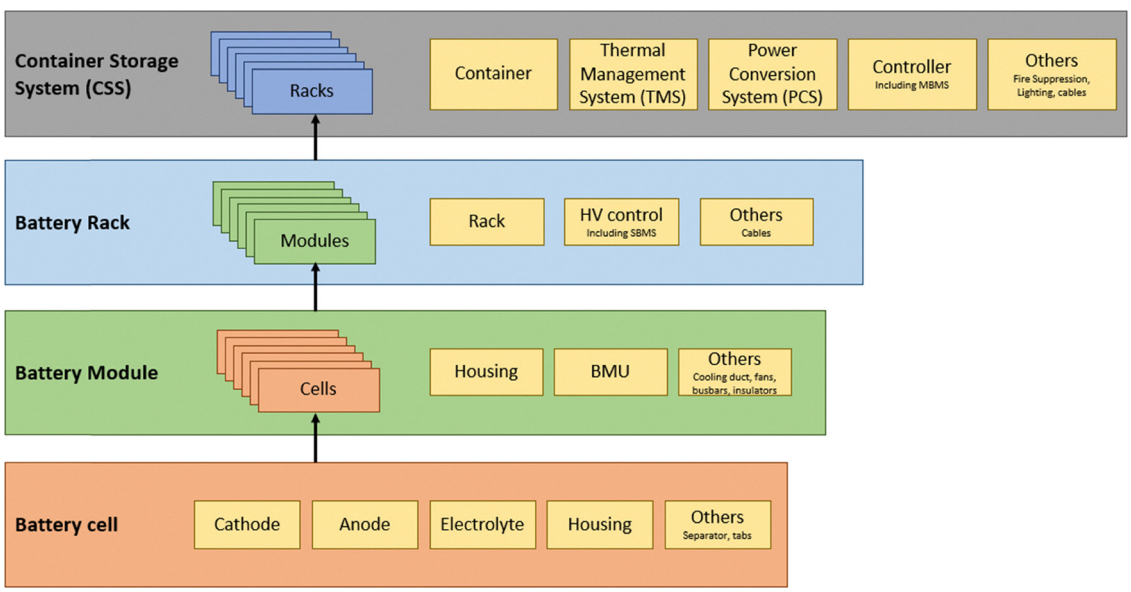

Fig. 2 Composition of a CSS. All components apart from the battery cells are considered balance-of-system (BOS) components. MBMS: master battery management system; SBMS: secondary battery management system; BMU: battery management unit. The figure is based on Andreasi-Bassi *et al.* (2025).[52]

the CSS incorporates a TMS. The configuration of the TMS depends on the chosen cooling approach, which in commercially available systems is generally limited to air- or liquid-cooling.[56,57]

Air-cooled designs typically employ several air-conditioning units in combination with fans integrated into the battery modules. In contrast, liquid-cooled systems include additional components such as a cooling unit, coolant circulation pipes, and cooling plates attached to the battery modules. Regardless of the overall cooling method, most electronic components are air-cooled, often assisted by built-in fans to enhance airflow.

The selection of a suitable TMS is primarily influenced by three factors: the system's heat output, the ambient environmental temperature, and any exceptional environmental conditions. In general, liquid-cooling offers superior heat dissipation and efficiency, making it more suitable for high-power or thermally demanding applications.[58] Air-cooling, by contrast, remains attractive for its simpler design, lower cost, and the absence of risks such as coolant freezing in low-temperature environments.[59]

2.2.3. Power conversion system (PCS). A power conversion system (PCS) serves as the interface between the battery modules and the power grid, enabling bidirectional energy transfer between the direct current (DC) and alternating current (AC) systems.[60] This is achieved through a combination of a transformer, an inverter, and a DC/DC converter, although the inverter and converter can also be integrated into a single bidirectional unit. The transformer connects the PCS's DC system to the power grid, ensuring that the CSS output matches the required AC voltage levels. When the grid voltage differs from the output of the AC/DC converter—such as in connections to local distribution or transmission networks—a transformer is essential to synchronize the output voltage with the grid.[50,60]

In a CSS, the PCS is generally implemented in one of two configurations: either as multiple PCS modules or as a single integrated PCS cabinet. In the latter configuration, the cabinet typically contains both the AC/DC and DC/DC converters, and in some cases, an integrated transformer. Systems employing a modular PCS design, by contrast, usually house the transformer in a separate cabinet located outside the container. The systems analyzed in this study utilize the modular PCS configuration. This has the advantage of providing more space for batteries in the container, resulting in higher energy density.

2.2.4. Controller and auxiliary system. Communication and data exchange within the CSS are centralized in the controller. Housed in a dedicated cabinet equipped with a control panel and display, the controller manages overall system operations and grid connectivity. It monitors and coordinates the status, protection, and communication among all major subsystems—including the PCS, BMS, heating, ventilation, TMS, and fire suppression systems. The controller also incorporates data storage capabilities, enabling operators to review historical data and diagnose operational issues. Its operating system is designed to integrate seamlessly with third-party Supervisory Control and Data Acquisition (SCADA) or Energy Management Systems (EMSs), supporting remote monitoring and control.

The auxiliary systems of the CSS include fire suppression, lighting, and cabling. The fire suppression system continuously monitors temperature, humidity, and gas levels inside the container. In coordination with the EMS, the controller processes these sensor signals and activates extinguishers, alarms, and sprinklers as needed to ensure effective safety responses. Lighting is provided by explosion-proof LED fixtures for routine operation, supplemented by emergency lights for use during power loss or emergency conditions.

Finally, due to its substantial weight, the CSS is typically installed on a reinforced concrete foundation. The foundation provides structural stability, prevents settling or sinking under heavy loads, and ensures resilience in severe weather. It is generally constructed on-site during installation, as most CSS units are deployed on land near photovoltaic (PV) plants and grid connection points where natural ground anchoring is insufficient.

2.3. Assessed systems

Based on the identified key components, two CSSs were modeled—one featuring an air-cooled and the other a liquid-cooled TMS. Both designs are derived from detailed manufacturer data sheets, supplemented with additional literature sources. Fig. 3 provides a visual overview of the modeled systems, while Table 2 summarizes their key specifications as described in the technical documentation.

Fig. 3 Graphical representation of a CSS. Pictures show an air-cooled system, which can be seen by the spacing between the battery racks (source: Power Sonic, Evesco, use with permission).[46]

The total energy capacities of the modeled systems are 2064 kWh with a power rating of 1000 kW for the air-cooled design, and 3008 kWh with a power rating of 1600 kW for the liquid-cooled design. Both are housed in 20-foot non-walk-in ISO shipping containers, featuring external access doors that allow maintenance and inspection of the battery racks and auxiliary components from outside. This compact layout enables efficient use of space and allows for higher energy density within the same container volume than a walk-in design CSS. The systems differ primarily in their cell configurations. The air-cooled CSS comprises six racks with 24 modules each, and each module contains 16 cells connected in series. The liquid-cooled CSS, in contrast, includes eight racks with eight modules each, and each module consists of 48 cells in series.

Both systems employ LIBs with LFP as the CAM. The LFP-based configuration serves as the reference for comparison with SIB systems. The SIB technologies analyzed are based on three representative CAM types: sodium manganese hexacyanoferrate (MnPBA) as a PBA, sodium vanadium fluorophosphate (NVPF) as a polyanionic material, and sodium nickel iron manganese oxide (NFM) as a layered metal oxide. The material compositions of the CAMs and the corresponding cell designs are based on the work of Voß *et al.* (2025).[61]

The cited work presents the latest cell models from SIBs alongside production data at an industry level. However, it should be emphasized that these are theoretical models of prismatic cells. Performance and resulting impacts can vary significantly when primary data are used. In a previous study, we also developed cell models of pouch cells with NVPF and MnPBA cell types in a laboratory setting.[62] These were based on measured and constructed LIB cells in the same laboratory. However, only significantly lower energy densities of 118–209 Wh L^{-1} could be achieved. Other studies also report lower energy densities than the study by Voß *et al.* (2025), at around 150–210 Wh L^{-1} for SIB cells.[61,63] Nevertheless, data from Voß *et al.* (2025) were used here, because they provide detailed LCI data on various SIB cell types based on a consistent modelling approach.[61] Furthermore, the high energy densities are consistent with industry reports, with Novonix announcing 272 Wh L^{-1} and CATL approximately 350 Wh L^{-1} for one SIB each.[64,65]

Because the CSS architectures are optimized for LFP cells, the specifications in Table 2 refer to the LFP-based model. To enable a direct comparison with SIB systems, it was assumed that SIB cells could be installed in the same physical configuration, occupying identical space within the racks. Consequently, the overall energy capacity of the SIB systems decreases proportionally to their lower volumetric energy densities. The ratio of SIB-to-LFP cell energy densities was used to determine the adjusted system capacities. Table 3 presents the relevant cell characteristics and the resulting total system energies for all examined chemistries.

2.4. Life cycle inventory (LCI)

This section provides a detailed description of the life cycle inventory (LCI) modeling process for the CSS. It covers the categorization of BOS components and their subassemblies, the identification of materials used in each main component, and the key modeling parameters and data sources applied. To ensure realistic system representation, the LCI model was developed based on the most prevalent design features and

Table 2 Key data of modeled CSSs based on LFP CAM

	Air-cooled system	Liquid-cooled system
Power/energy capacity	1000 kW/2064 kWh	1600 kW/3008 kWh
Rated voltage	1228.8 V	1228.8 V
Dimension and style	20 ft/non walk-in container	20 ft/non walk-in container
Weight	24 t	28.5 t
Battery chemistry	LFP (3.2 V/280 Ah)	LFP (3.2 V/306 Ah)
Cell configuration	16s1p	48s1p
Number of battery racks (capacity)	6 racks (344.064 kWh)	8 racks (376.01 kWh)
Weight of battery rack	2910 kg	2540 kg
Number of battery modules per rack (capacity)	24 modules (14.33 kWh)	8 modules (47 kWh)
PCS design	Modular PCS per rack	Modular PCS per rack

Table 3 Battery cell and resulting system characteristics for all cell types investigated (air|liquid-cooled). Cell data (lines 1 and 2) are taken from Voß *et al.* (2025)[61]

		LFP	MnPBA	NVPF	NFM
Specific energy	[Wh kg^{-1}]	176.6	142.2	152.2	160.5
Energy density	[Wh L^{-1}]	426.0	255.2	309.5	344.0
Volumetric density ratio to LFP		1	0.5991	0.7265	0.8075
Energy per (air-cooled|liquid-cooled)					
Module	[kWh]	14.33|47.00	8.59|28.16	10.41|34.15	11.57|37.95
Rack	[kWh]	344|376	206|225	250|273	278|304
System	[kWh]	2064|3008	1236|1802	1500|2185	1667|2429

LFP: lithium iron phosphate, MnPBA: sodium manganese hexacyanoferrate, NVPF: sodium vanadium fluorophosphate, NFM: sodium nickel iron manganese.

technologies currently available on the market and the production is assumed to take place in China. This approach enables a comprehensive and up-to-date assessment of the material composition and environmental impacts associated with modern CSS configurations.

2.4.1. Battery racks. Battery racks were modeled using data from several publications, with the battery cell inventories derived from the most recent and comprehensive study on SIBs by Voß *et al.* (2025).[61] This source provides detailed LCI data for multiple SIB chemistries, from which three CAMs were selected—one representative of each major type, as previously discussed. All three SIB variants employ hard carbon, produced from pitch, as the anode material, reflecting the base-case configuration in the cited study. Aluminum foil serves as the current collector on both electrodes, and sodium hexafluorophosphate ($NaPF_6$) is used as the electrolyte.

The reference LIB model, based on LFP, also follows the dataset by Voß *et al.* (2025), to ensure comparability.[61] It includes graphite as the anode material, copper foil as the anode current collector, and lithium hexafluorophosphate ($LiPF_6$) as the electrolyte. Particular attention is given to the modeling of synthetic graphite production, as recent research indicates that the environmental impact of battery-grade synthetic graphite has historically been underestimated.[66] In this study, the Acheson powder route—currently considered the state-of-the-art production process—is applied, as implemented in the latest version of ecoinvent 3.11. The assumed ratio of natural to synthetic graphite corresponds to the default process composition in the database (35% natural and 65% synthetic).

The energy demand for cell manufacture is modeled following Degen *et al.* (2023), representing large-scale (gigawatt-level) production facilities.[67] The production of LFP cells requires 18 kWh electricity and 19 kWh natural gas per kWh of battery capacity, while SIB production requires 11 kWh electricity and 12 kWh natural gas per kWh of capacity. Further methodological details and the full inventory are provided in the cited studies and summarized in the SI. Looking beyond the cell, the battery module is modeled based on Baumann *et al.* (2020), which provides detailed LCIs for rack-mounted battery trays used in stationary storage systems.[68] The model was adjusted according to the module weights specified in the manufacturers' data sheets. The mass of the rack housing and cables is derived from Da Silva Lima *et al.* (2021), assuming that the rack housing accounts for 17% of the total weight of a single battery rack and the cabling represents 0.705% of the total.[14] The HV control box is represented using the ecoinvent process "electronics, for control units".

2.4.2. Container and thermal management system (TMS). The container model is based on the 20-ft intermodal shipping container dataset from ecoinvent. Its interior walls are lined with flame-retardant insulation layers, consisting of a cement board, an orientated strand board, and polyurethane, applied in specific zones according to McKinnon *et al.* (2022), a study on fire protection for LIB ESSs.[69]

LCI data for the air-cooling TMS were derived from the EPD of a 3.6 kW, 37 kg unit.[70] The system was scaled using a manufacturer's reported air conditioning power demand of 25 kW for a 500 kW/1000 kWh system.[71] When scaled to the underlying 1000 kW and 2064 kWh systems by a factor of two and combining that with the correlation of power and weight of approximately 10 kg kW^{-1} derived from the TMS LCI data available, the air-cooling system including indoor and outdoor units is assumed to weigh 514 kg with a power of 40 kW. Battery modules additionally include fans and Al heat sinks for improved heat transfer. Further details are provided in the SI.

The liquid-cooling TMS follows the design of the 500 kWh liquid-cooled lithium battery energy storage unit in the study by Guo *et al.* (2023).[56] This includes an aluminum cooling plate integrated into the modules for heat exchange, with coolant circulating through external inlets/outlets connected to nitrile rubber hoses and copper pipes. Pipe size and count are derived from Xian *et al.* (2025) and adjusted to system dimensions.[72] The coolant is a 50 : 50 ethylene glycol and deionized water mix with a total mass of 126 kg. At the circuit level, cooling is provided by a 40 kW unit composed of a condenser, an evaporator, a compressor, a pump, and a PTC heater. Its LCI is based on the BoM of a water-cooled vapor-compression chiller from Catrini *et al.* (2018), scaled linearly to 40 kW, yielding $\approx$160 kg (excluding casing and PTC).[73,74] Three auxiliary 5 kW heaters and a pump are added from ecoinvent. The pump was downsized on the basis of weight-to-power conversion to align with the required performance specifications. For container-level thermal management, especially for BOS components, a liquid-cooled CSS also includes one air conditioning unit. Therefore, one 3.6 kW unit was included, modeled analogously to the air-cooled case.

2.4.3. Power conversion system (PCS). Both the air-cooled and liquid-cooled CSSs are equipped with one bi-directional AC/DC PCS module per battery rack. Each module provides 200 kW power and weighs approximately 100 kg. The two CSSs are modeled using identical LCI data, differing only in the number of PCS modules installed. The composition of the PCS modules is based on the LCI of an inverter for a home storage system (HSS), as reported in a previous study.[12] It is adapted to the bigger size, and its share of steel, representing the casing, is reduced from 45 wt% to 27 wt%.

The transformer LCI is derived from Hunziker *et al.* (2020), which provides a detailed inventory for a conventional line-frequency transformer (LFT) with an on-load tap changer (OLTC), commonly used in PV power plants.[75] The reference transformer in the cited study is rated at 630 kVA with a total mass of 2666 kg. For the CSS in this study, higher-rated transformers are required: 1200 kVA for the air-cooled system and 1800 kVA for the liquid-cooled system. These ratings include a power factor of approximately 0.9, as well as thermal and overload margins to prevent overheating. Scaling was performed based on commercially available transformers of the required ratings and their reported weights. For instance, commercially available 1200 kVA and 1800 kVA transformers weigh approximately 4.1 t and 5.5 t, respectively, including tanks, accessories, and oil.[76,77]

The weight distribution of transformer components closely matches the shares reported by Hunziker *et al.*; for example, the

tank and accessories constitute 36 wt% according to the manufacturer and 31 wt% in the study. Therefore, the composition per kg of transformer mass was modeled according to the study by Hunziker *et al.* (2020).[75] Full details of the transformer composition are provided in the SI.

2.4.4. Controller and auxiliary system. Both CSSs are assumed to use the same controller design. According to the data sheet of the liquid-cooled system, the controller weighs approximately 30 kg. Its composition is based on the LCI of a HSS controller, as reported in a previous study.[12]

The concrete foundation is sized according to the base area of a 20-foot container (6.06 m × 2.43 m), with a 20 cm extension on each side and a depth of 1 m, consistent with observations from a field visit. Assuming a concrete density of 2400 kg m^{-3}, the total mass of the foundation is 43.9 t. The fire suppression system incorporates standard components sourced from multiple manufacturers. Each container is equipped with two smoke detectors, two temperature detectors, and one combustible gas detector. The system further includes a fire control panel, audible and visual alarms, two fire sprinklers, and two 12 kg fire extinguishers using HFC-134a as the extinguishing agent, connected *via* steel fire pipes. All LCI data for the controller, foundation, and fire suppression system are provided in the SI.

2.4.5. Use phase. The environmental impacts occurring during the use phase of CSSs are associated with operational energy losses, which include round-trip efficiency (RTE) losses in the electrochemical cells, conversion losses, cooling energy demand, stand-by electricity consumption and electricity consumption of system electronics. However, detailed operational data on all these aspects are generally not made available in the literature, nor are they disclosed by manufacturers or system operators. Attempting to estimate all missing parameters would require numerous assumptions, resulting in high overall uncertainty.

Therefore, this study takes a simplified approach, quantifying use-phase impacts by applying an overall system level RTE. In line with literature values, a system efficiency of 85% and 90% for operation at 1C for one cycle per day for air- and liquid-cooled systems is assumed, respectively. For grid-connected LIB systems, literature values range from 85% to 95%.[78–83] For SIBs, the same RTE values are assumed as for LIBs, as SIBs are capable of achieving comparable round-trip efficiencies to LIBs under typical operating conditions.[84,85] For the calculation of the impacts, the ecoinvent process ''electricity production, photovoltaic, 570 kWp open ground installation, multi-Si|electricity, low voltage|cutoff, U - DE'' was used with the impact factors of about 0.1004 kg CO_2 eq. per kWh and 4.19 × 10^{-6} kg Sb eq. per kWh for the impact categories GWP and mineral resource use, respectively.

The main variables of the use phase investigated in this study are the applied C-rate and the number of cycles per day, with a significant influence on system efficiency. The range for the C-rate was chosen from 0.25C to 2C and for cycles 0.5 to 1.7, reflecting the most common use cases and the system limits. The depth of discharge was kept constant at 80% over the course of 20 year lifetime assumed for both systems.

Further system efficiencies are strongly influenced by the cooling method of the system, as liquid-cooling is generally more energy efficient than air-cooling. Akbarzadeh *et al.* (2021) demonstrated that, for a cooling power consumption of around 0.5 W, the average temperature of the hottest battery cell in a liquid-cooled module can be approximately 3 °C lower than in an air-cooled module.[58] This is due to the lower thermal conductivity and heat capacity of air which can also lead to poorer peak temperature control and less uniform temperature distribution, unless implemented with very high airflow rates and complex ducting.[86] Air-cooling is thus considered adequate only for low-to-moderate dissipation loads, whereas it is insufficient for applications with C-rates exceeding 1C, as confirmed also by expert judgment.[87] For this reason, liquid-cooled systems are expected to achieve higher round-trip efficiencies compared to air-cooled systems.

Table 4 shows the system round-trip efficiencies of both systems. On the left is the air-cooled system, for which the 2C rate was excluded due to infeasibility. On the right is the liquid-cooled system. It should be noted that the capacity decrease of the battery cells over the lifetime was not taken into account as the use phase is not the focus of this study and would require an analysis of cell type-specific capacity retention.

2.4.6. End-of-life phase. The EOL phase is modeled using an EOL recycling approach with crediting, in which materials recovered from recycling are assumed to substitute equivalent materials from the market. Accordingly, credits are assigned for the avoided production of partly primary materials. A detailed description of the EOL approach can be found in the SI. The recycling processes are assumed to take place in Germany, using an up to date electricity mix for the LCI modeling, stemming from a former work.[62]

The recycling processes of the three main metals of the periphery, aluminum, copper and steel, are each represented through two processes: (i) the production of secondary materials from scrap, capturing the recycling efforts; and (ii) the corresponding market process as an ''avoided product'' output, providing the credit. The amounts for both processes are equally defined by the production processes for secondary materials, as the amount of scrap material used differs depending on the material, and the recycling process should represent the treatment of 1 kg of scrap material. This modeling approach generally leads to negative environmental impacts and therefore a reduction in total environmental impacts. However, the recycling processes themselves—through energy

Table 4 System round-trip efficiencies dependent on the number of cycles per day and C-rates (air|liquid-cooled). The base case of 1 cycle per day and a rate of 1C is marked in bold. Values are based on expert judgement

	C/4	C/2	1C	2C
0.5 cycles	86%|90%	85%|89%	83%|88%	—|78%
1 cycle	88%|92%	87%|91%	**85%|90%**	—|80%
1.5 cycles	89%|93%	88%|92%	86%|91%	—|81%
1.7 cycles	89%|93%	88%|92%	86%|91%	—|81%

consumption, emissions, or waste generation—can in some cases lead to a net increase in specific impact categories. In addition to the three named metals, various plastics account for a significant proportion of several components and therefore their treatment process is described briefly below. For plastics, an incineration process with energy recovery is modeled based on the ecoinvent dataset, as it represents the current method of handling mixed plastic waste. A similar approach is applied to the wooden insulation panels, which are first shredded into chips prior to incineration with energy recovery. The cables are separated into their constituent plastic and copper parts, which are then treated separately, as described above.

In addition, the recovery of high-impact metals such as gold, silver, palladium, and copper from the treatment of used printed wiring boards (PWBs) is included, as specified in the modeling rules established by the Joint Research Centre (JRC) of the European Commission for calculating the carbon footprint of industrial batteries.[52] The recycling efforts for PWBs include infrastructure, energy consumption and an estimation of the efforts for transportation. The credits for metal recovery are calculated by the multiplication of the amount of the corresponding material used in the PWB with a recycling rate which, according to Xue *et al.* (2015), amounts to 97%, 98%, 93% and 100% for gold, silver, palladium and copper, respectively.[88] These rates are specifically and only used for the recycling of the PWBs and are difficult to verify as data on the recycling of PWBs are difficult to obtain.

The EOL of most BOS components is modeled using these main components, while manual dismantling is not included in the efforts. This particularly includes all electronic devices such as the controller and the HV control box, which comprise the two upper levels of the BMS, consisting mainly of metals, plastics, cables and PWBs. Here, the mass fractions were taken from the production processes and recycled accordingly as described above. The EOL of the battery modules without the cells was also modeled accordingly. Where necessary, the treatment process was supplemented by component-specific recycling, some of which are described briefly below. The fire extinguisher tank is assumed to be reused elsewhere and is therefore excluded from recycling. Furthermore, the recycling of the secondary coolant (ethylene glycol–water mixture) in the liquid-cooled system is modeled based on a glycol recycling report.[89] All details of the LCI of all EOL processes are provided in the SI.

For the battery cells, a combined pyrometallurgical–hydrometallurgical recycling route is assumed, also following the carbon footprint rules for industrial batteries.[52] This modeling approach includes the recovery of current collector metals but excludes the recovery of active materials and electrolytes. Therefore, there is no credit for the recovery of lithium, graphite or hard carbon. A battery collection rate of 100% is assumed. The individual recycling processes are not analyzed further in this study, as they are outside the main scope; detailed descriptions can be found in the referenced report.

In addition to the final treatment, EOL modeling also includes consideration of the service life of the components.

Table 5 Assumptions regarding the lifetime of battery cells

		LFP	MnPBA	NVPF	NFM
Lifetime (years)		15	15	15	15
Repl. factor (cal.)		1.33	1.33	1.33	1.33
Lifetime (cycles)		7000	7000	5000	4000
Repl. factor (cycl.)	0.5	0.52	0.52	0.73	0.91
	1	1.04	1.04	1.46	1.83
	1.5	1.56	1.56	2.19	2.74
	1.7	1.77	1.77	2.48	3.10
Repl. factor (effective)	0.5	1.33	1.33	1.33	1.33
	1	1.33	1.33	1.46	1.83
	1.5	1.56	1.56	2.19	2.74
	1.7	1.77	1.77	2.48	3.10

Sources: Peters *et al.* (2021)[84] for calendrical lifetime and Zhang *et al.* (2024)[95] for cyclical lifetime.

This applies to both the battery cells and the BOS components. With an operating life of 20 years for the entire system, most BOS components can be used for the entire period, as they will have a service life of at least this length. This applies not only to the container, the transformer and the cables, but also to the controller and the air-cooling system.[90–93] The only two components that have a lower expected service life than 20 years are the liquid-cooling system and the inverter, each with 15 years.[93,94] To account for this, a theoretical replacement factor is calculated by dividing the operating time by the expected service life. The impact of the components is then multiplied by the factor, which is 1.33 for both of the components mentioned.

With regard to the cells, in addition to the calendrical lifetime, a cyclic lifetime must also be taken into account. Depending on which limit the cell reaches first, the cyclical or calendar lifetime, the replacement factor applies. Thus, the higher of the two factors becomes effective. For the cyclical replacement factor, the number of cycles the cells go through per day is also crucial, as more cycles mean more frequent replacement. Table 5 shows the assumptions for the lifetimes of the various cells and the resulting replacement factors, based on recent scientific findings.[84,95] In this work, the service life of a battery cell is considered to end when 80% of its capacity remains.

3. Results

3.1. Cradle-to-gate

The cradle-to-gate environmental impacts for CSS production are provided in Fig. 4 and 5, corresponding to the impact categories GWP and mineral resource use, per kWh of storage capacity, respectively. Both figures compare the four cell types, each integrated into an air-cooled and a liquid-cooled system configuration. The results in all other impact categories can be found in the SI.

Consistent trends can be seen for all cell types in both impact categories: liquid-cooled systems have a lower environmental impact than air-cooled systems. This reduction is primarily due to the higher packing density that can be achieved in liquid-cooled systems, since no additional spacing is required for air circulation between battery modules.

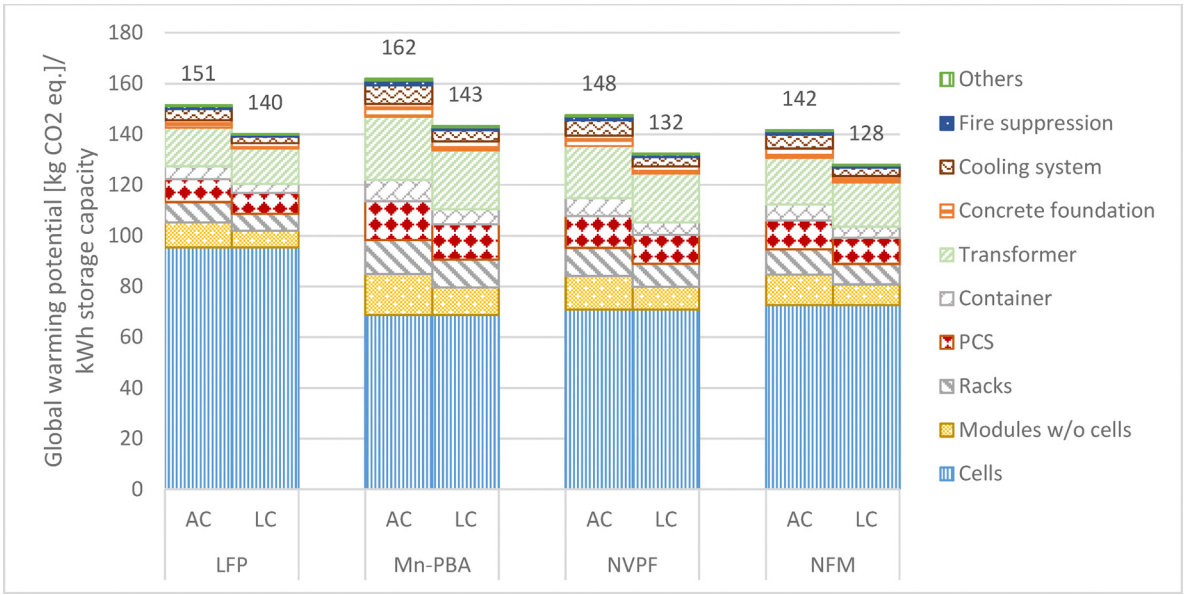

Fig. 4 Global warming potential of air-cooled (AC) and liquid-cooled (LC) CSSs from cradle to gate. Balance-of-system (BOS) components include everything except cells. Values are given per kWh storage capacity.

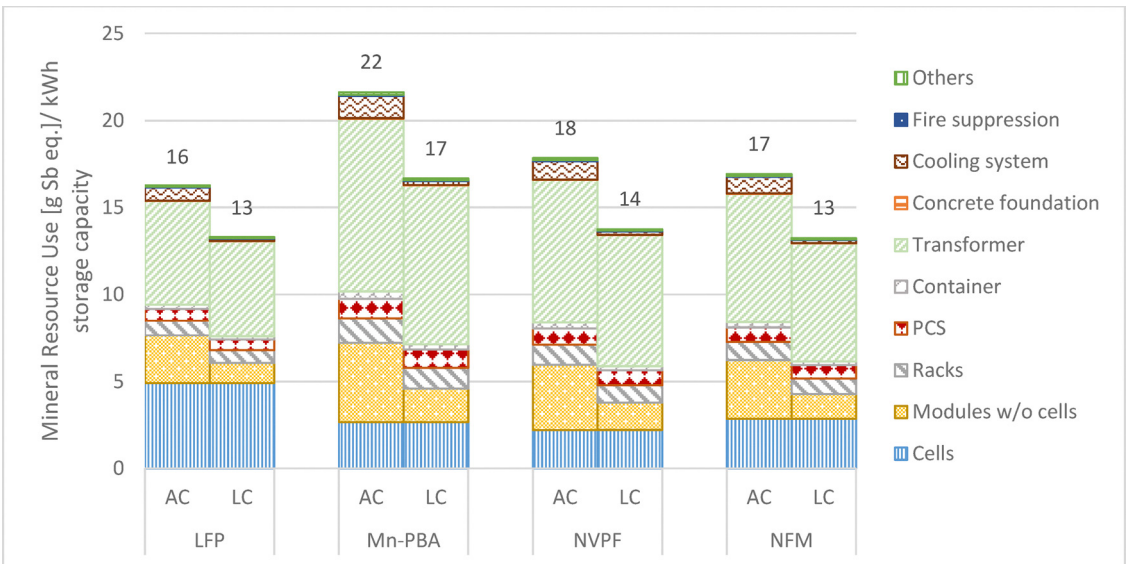

Fig. 5 Mineral resource use, minerals and metals of air-cooled (AC) and liquid-cooled (LC) CSSs from cradle to gate. Balance-of-system (BOS) components include everything except cells. Values are given per kWh storage capacity.

Consequently, the total system capacity increases, thereby reducing the environmental impact per unit of storage capacity. The impact range among the cell types is relatively small. For GWP, NFM-based systems have the lowest impact, reaching approximately 89% of that of the MnPBA-based configuration, the highest-impact system. A similar trend is observed for mineral resource use, although the differences are more noticeable: the LFP-based system shows the lowest impact, accounting for around 75–80% of the MnPBA system's impact. These variations are primarily explained by differences in cell energy density, which influence the total system storage capacity and thereby affect normalized impact values.

BOS components account for a substantial proportion of total impacts, representing 32–58% of GWP and 63–88% of mineral resource use. This contribution is generally higher for SIB-based systems than for LFP-based systems. This is because SIB cells have a lower energy density, resulting in reduced system capacities. Since impacts are expressed per kWh of capacity, the BOS contribution is relatively larger in these configurations. The same effect is observed when comparing air-cooled and liquid-cooled systems.

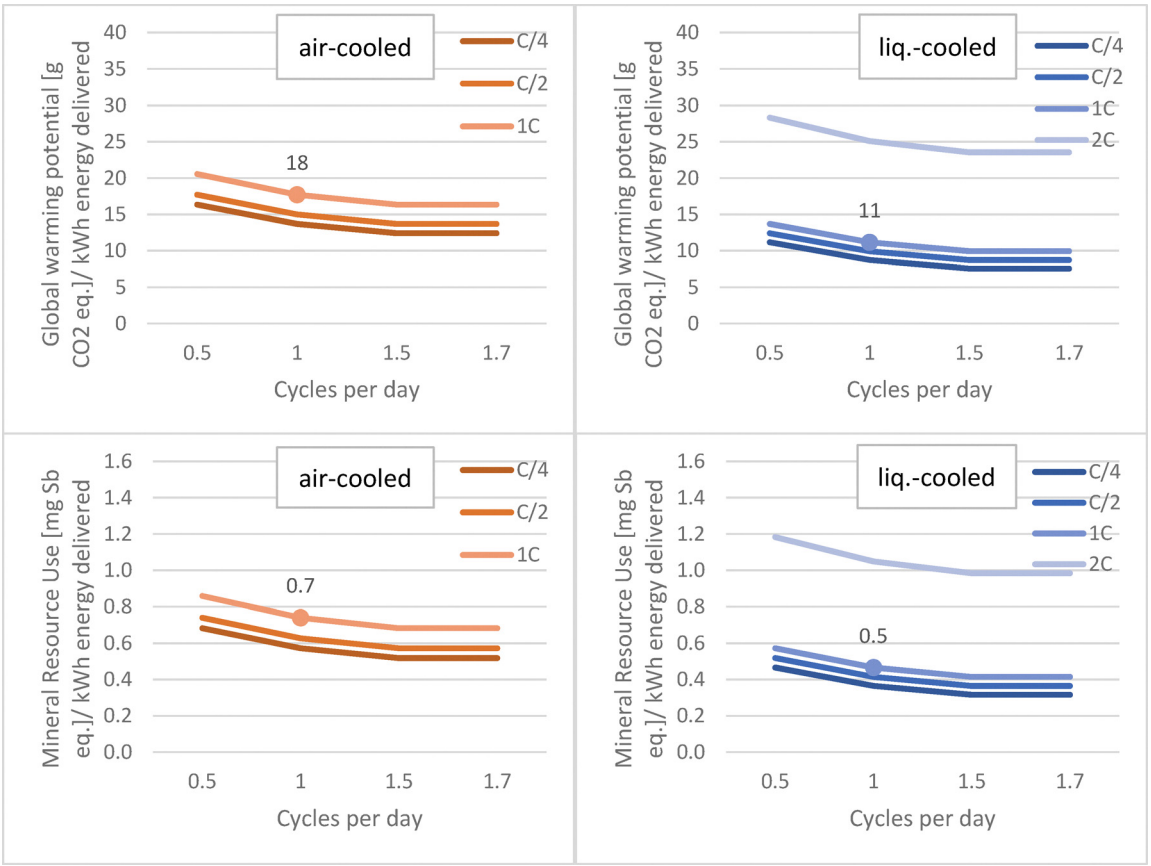

Fig. 6 Total environmental impacts of the use phase depending on the C-rate and cycles per day. Red: air-cooled system; blue: liquid-cooled system. Values are given per kWh energy delivered. The base case of 1 cycle per day and a rate of 1C is marked explicitly.

Furthermore, the increased packing density of liquid-cooled systems, especially at the module level (*e.g.*, 14 kWh per module for an air-cooled LFP system *versus* 47 kWh per module for a liquid-cooled LFP system), leads to a significantly lower environmental impact from module housings, including module electronics. Notably, PWBs in the module assembly contribute substantially to mineral resource use, almost exclusively due to the presence of gold. With respect to the cooling subsystem, the GWP impacts are similar for air-cooled and liquid-cooled configurations. However, notable differences arise in mineral resource use. Air-cooled systems show significantly higher material impacts, primarily due to the extensive use of copper in the air conditioning unit, particularly in its outdoor components.

3.2. Use phase

The impacts attributable to the use phase of the CSS, which is assumed to take place in Germany, are displayed in Fig. 6. The results are shown for the air-cooled system on the left and for the liquid-cooled system on the right for the impact categories GWP (top graphs) and mineral resource use (bottom graphs). The energy lost over the lifetime is calculated by multiplying the total energy supplied by the reciprocal value of the overall RTE rates, shown in Table 4. The used impact factors are approximately 0.1004 kg CO_2 eq. per kWh and 4.19×10^{-6} kg Sb eq. per kWh for the impact categories GWP and mineral resource use, respectively. As the efficiencies are assumed to be identical for all cell types and the results are given per kWh energy delivered, they are identical and therefore only presented once in Fig. 6.

The impacts are shown for different C-rates and a varying number of cycles per day on the *x*-axis. It should be noted that a C-rate higher than 1C is not feasible for an air-cooled system, as the heat generation cannot be handled by such a system. It can be observed that the impacts are higher with increasing C-rate, as heat generation and therefore the cooling efforts increase. However, when the cycles per day increase, the impacts decrease per kWh energy delivered, as the system has a higher capacity utilization. The liquid cooled system shows lower impacts due to a higher RTE, attributable to higher cooling efficiency compared to air-cooling. In the further presentation of results, the base case of 1 cycle per day and a rate of 1C is used. For this reason, the value for this case is shown explicitly, which also makes the comparison between the two systems more tangible.

3.3. End-of-life phase

The EOL phase leads to an overall reduction of the environmental impacts of the CSS, primarily due to material recovery through recycling. The impacts for all components are shown

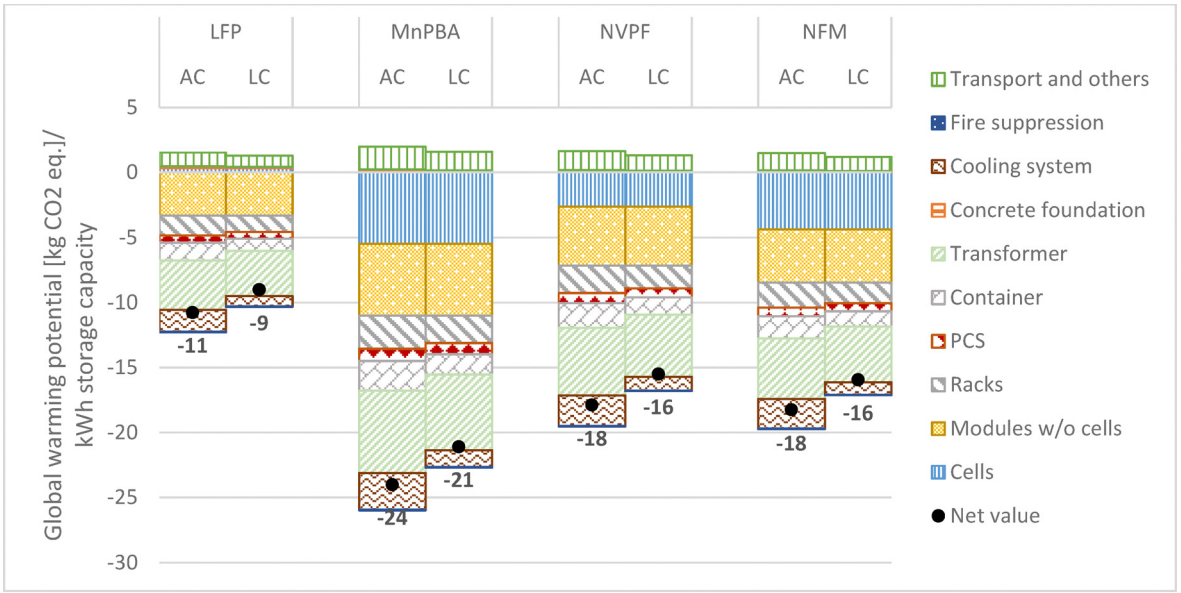

Fig. 7 Global warming potential of the EOL phase of air-cooled (AC) and liquid-cooled (LC) CSSs. Balance-of-system (BOS) components include everything except cells. Values are given per kWh storage capacity.

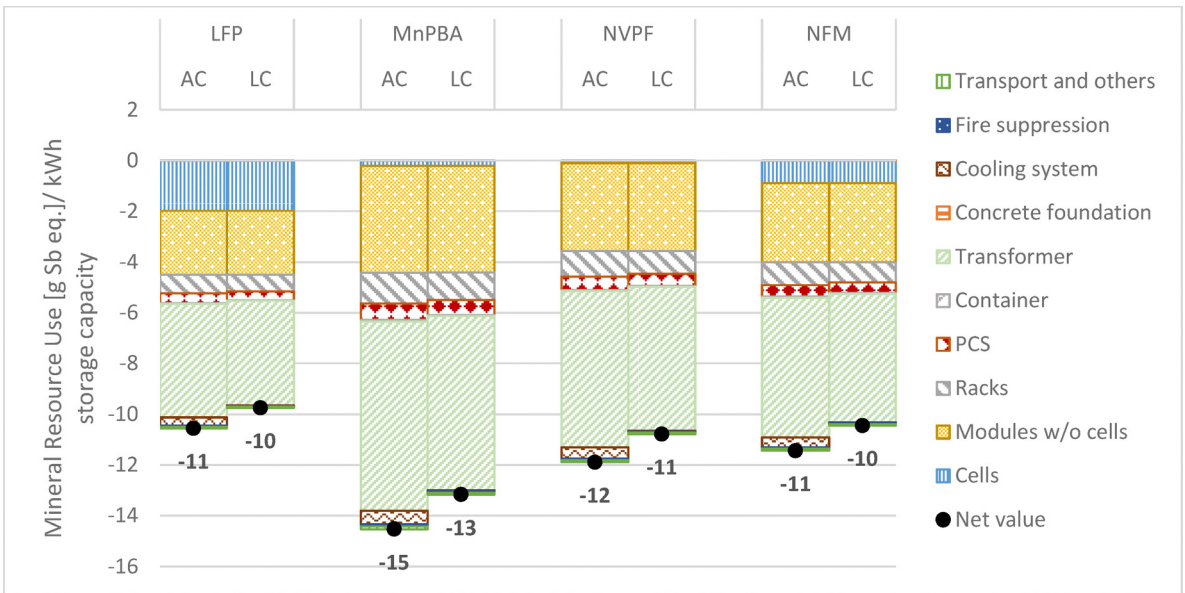

Fig. 8 Mineral resource use, minerals and metals of the EOL phase of air-cooled (AC) and liquid-cooled (LC) CSSs. Balance-of-system (BOS) components include everything except cells. Values given per kWh storage capacity.

in Fig. 7 and 8. Generally, it can be observed that the recycling benefits of systems with lower energy density are more prominent, *e.g.*, for the MnPBA system, given that the results are expressed per kWh of storage capacity. While the absolute recycling potential is comparable across systems, the smaller capacity of low-density systems increases the relative benefit. This is consistent with the production-phase pattern, where the same scaling effect resulted in higher BOS contributions. Consequently, air-cooled systems, which typically exhibit lower capacities than liquid-cooled ones, demonstrate slightly higher relative recycling benefits.

At the system level, the majority of components contribute positively to this reduction, with the transformer providing the most significant benefit in both impact categories. For GWP the transformer accounts for 26–39% of the total savings, which is attributable to the high recyclability of its metallic content. In contrast, additional impacts in terms of GWP arise from transport processes required to collect and deliver components for recycling. At the cell level, only the recycling of metallic current collectors results in a net reduction in GWP; however, these benefits are partially offset by the energy and process

requirements of the recycling operations. The overall effect is comparable across chemistries, although higher-energy-density systems involve heavier cells and therefore greater recycling efforts per kWh. The cooling systems themselves contribute marginally to the overall EOL balance, and both air- and liquid-cooled configurations achieve similar net benefits.

A similar pattern is observed for mineral resource use. The transformer, once again, is the primary contributor to the benefits, accounting for approximately 42–52% of the total. Among the cell types, only LFP and NFM systems demonstrate a clear benefit from cell recycling; in the case of LFP the copper from the cathode current collector can be effectively recycled, and in the case of NFM the recovered nickel gives significant credits. Conversely, MnPBA and NVPF systems yield negligible recycling benefits, as only the aluminum current collector is assumed to be recovered. Moreover, the recycling of PWBs in the battery modules offers a substantial advantage through the recovery of high-impact metals, primarily gold. This effect is again particularly apparent in systems with a lower overall capacity, where the relative contribution of these components per kWh is higher.

3.4. Full life cycle

The full LCA results are presented for operation at a rate of 1C and one cycle per day in Fig. 9 and 10, representing typical conditions for stationary energy storage applications. In addition to the production, use, and EOL phases, the results also include replacement efforts, accounting for the environmental burden associated with component replacement during the system's operational lifetime. It is important to note that the extent of cell replacement is dependent upon the definition of the use phase, particularly the assumed number of equivalent full cycles. Additional factors such as the C-rate, temperature, and state of charge can significantly influence battery degradation and thus replacement needs. These effects are not explicitly modeled in this study but are acknowledged as sources of uncertainty.

When considering the full life cycle, all systems exhibit comparable environmental impacts. However, liquid-cooled systems consistently achieve lower overall impacts than air-cooled systems in both impact categories, primarily due to their higher total storage capacity, which reduces normalized impacts per kWh energy delivered. Across both cooling concepts and chemistries, the production phase remains the dominant contributor to total impacts, accounting for 48–82% of the overall burden. The relative contribution is higher for mineral resource use and lower for GWP. Among the chemistries considered, NFM systems show the highest replacement impacts, primarily due to their relatively low cycle life. Across all systems, 80–95% of the total replacement impacts in both GWP and mineral resource use categories stem from the cells themselves.

The role of the EOL phase varies depending on the impact category. For GWP, the net benefits from recycling are comparatively small, as the recycling processes themselves require energy and thus generate additional emissions. In contrast, the benefits for mineral resource use are substantial, compensating 47–64% of the production-related impacts. This substantial reduction can be attributed to the effective recovery of metals and the prevention of primary material extraction. In particular, the recycling of copper and the recovery of high-impact metals such as gold from the PWBs in the battery modules play an important role in reducing the overall resource demand of the CSS.

3.5. Sensitivity analysis

The sensitivity analysis investigates the effect of varying one key operational parameter, the average number of cycles per day, on the total environmental impacts of the CSS. All CSSs were

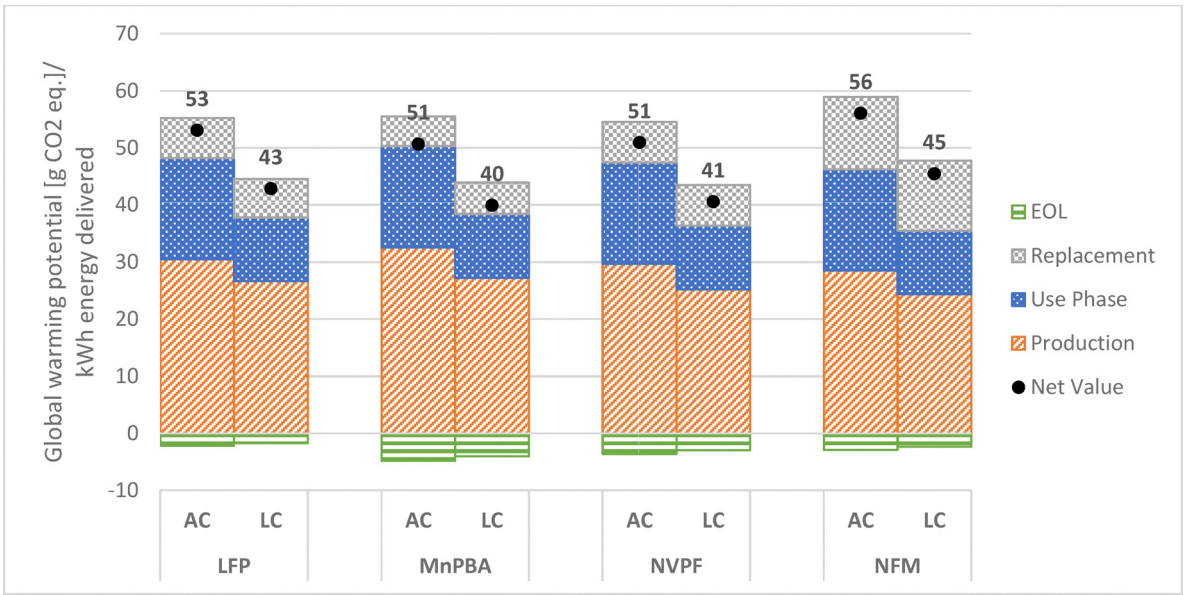

Fig. 9 Global warming potential of the full life cycle (1C, 1 cycle) of air-cooled (AC) and liquid-cooled (LC) CSSs. Values given per kWh energy delivered.

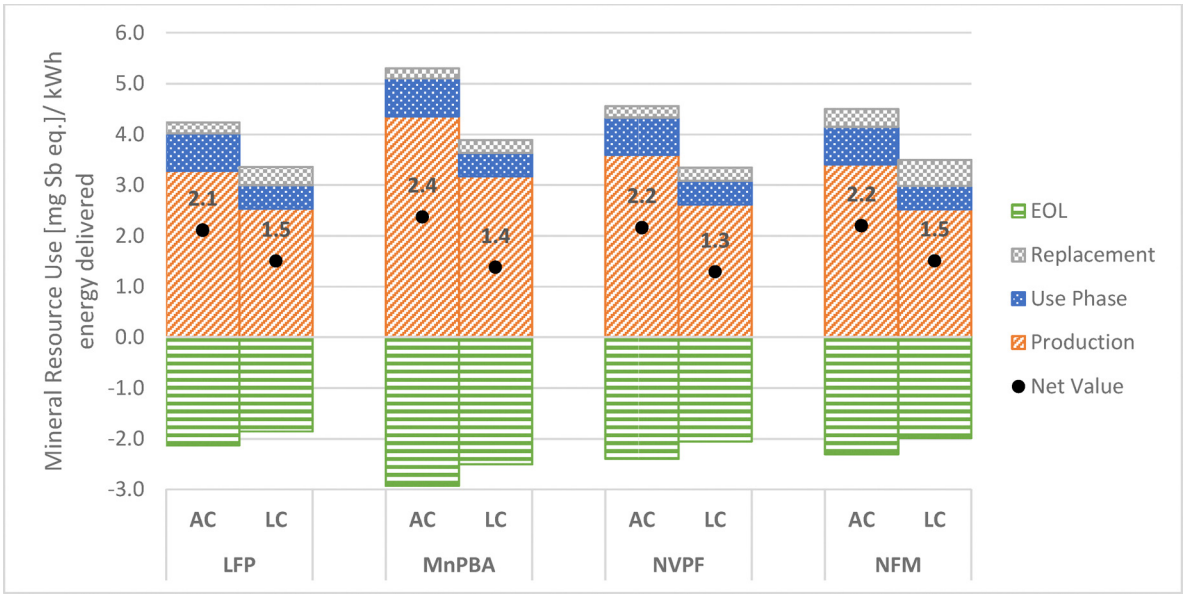

Fig. 10 Mineral resource use, minerals and metals of the full life cycle (1C, 1 cycle) of air-cooled (AC) and liquid-cooled (LC) CSSs. Values given per kWh energy delivered.

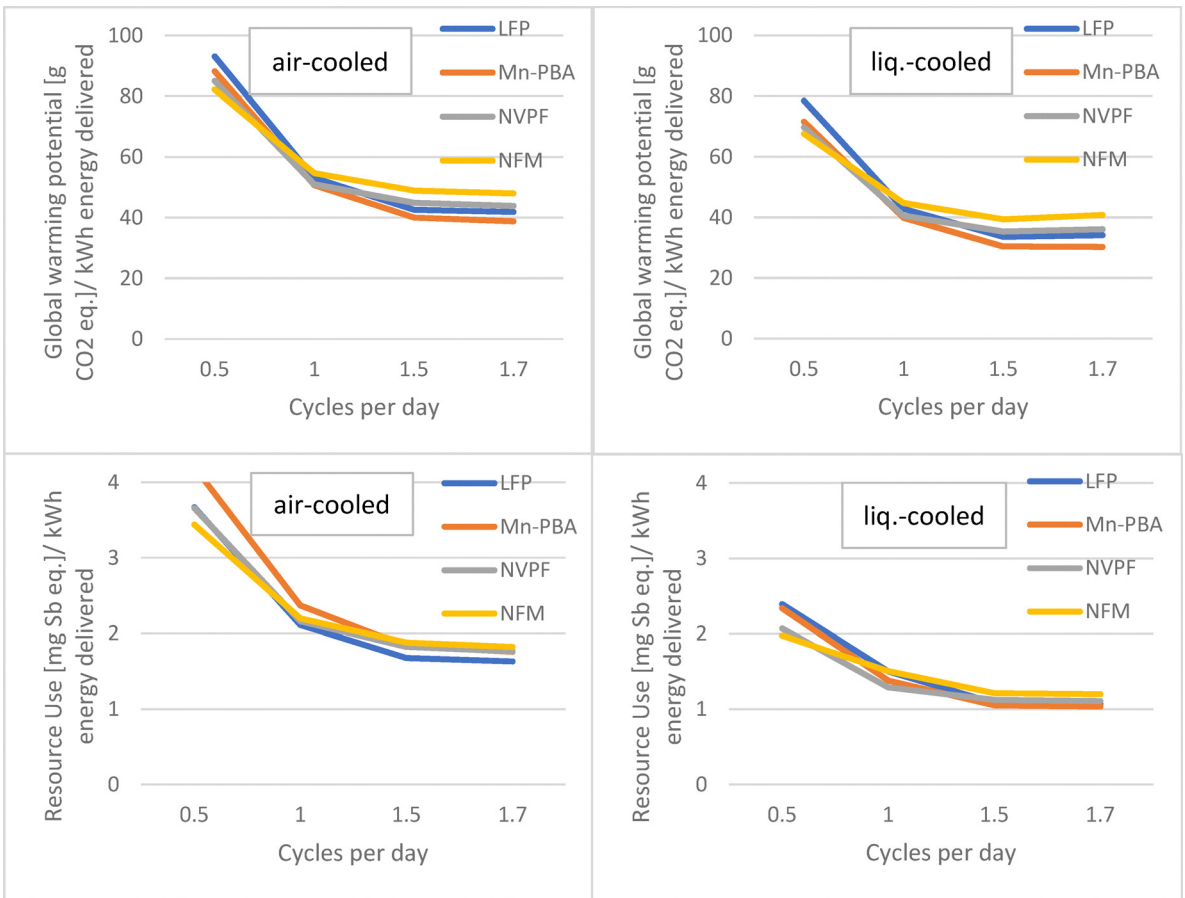

Fig. 11 Sensitivity analysis of full life cycle impacts with varying numbers of cycles per day, at a rate of 1C. Values given per kWh energy delivered.

modeled at a constant rate of 1C, with the results displayed per kWh of energy delivered in Fig. 11. The impacts for the air-cooled systems are presented on the left side, and those for the liquid-cooled systems on the right.

Across all CSSs and in both impact categories, a consistent trend is observed: environmental impacts decrease significantly as the number of daily cycles increases. This reduction is primarily driven by the higher total energy output over the system's lifetime, which increases the divisor used for normalization and thereby dilutes the fixed impacts, *i.e.*, those from production.

However, it is important to note that the rate of improvement diminishes as the frequency of cycling increases. Therefore, the decline in impacts is more pronounced when transitioning from 0.5 to 1 cycle per day than from 1 to 1.5 cycles per day. This non-linear behavior can be explained by the fact that only production-related impacts decrease proportionally with increased energy throughput, while use-phase impacts are only slightly affected by improved efficiencies. Conversely, replacement impacts generally increase with increased cycling frequency, as higher usage accelerates cell degradation and results in additional replacements. The effects of EOL follow a similar trend to those of production-related impacts, but enhance the effect, with a decrease of benefits at higher throughputs due to the effects of normalization.

As the cycle numbers increase, the NFM-based system demonstrates significantly higher impacts in comparison to the other chemistries. This is attributable to its limited cycle life, which results in a greater number of replacements being required. Despite these variations, the overall results show that all systems remain within a comparable impact range across the different cycling scenarios. Liquid-cooled systems consistently perform better than air-cooled ones due to their higher effective storage capacities.

4. Discussion

Overall, the results show rather comparable environmental impacts for sodium and lithium based CSSs, despite differences in energy density and material composition. While SIB cells exhibit slightly lower impacts in both GWP and mineral resource use compared to the LFP cell, their lower energy density results in higher relative contributions from BOS components when normalized per kWh of storage capacity. Additionally, liquid-cooled systems consistently achieve lower impacts than air-cooled ones across all chemistries and both impact categories. This improvement is mainly driven by higher packing density and system capacity, reducing the number of modules and BOS components needed per kWh of energy capacity. This underlines the importance of considering the entire system rather than the cell alone when assessing the environmental performance of large-scale storage systems.

The production phase and therefore the system composition are shown to be decisive factors for the overall environmental performance. Among the BOS components, the transformer contributes the largest share to total impacts, mainly due to the high use of copper and steel. In the mineral resource use impact category, the impact is even greater than that attributable to the battery cells. This is particularly striking in the case of SIBs, which use few rare metals and have lower energy densities, thereby further increasing the impact of BOS components. However, these effects can be offset by efficient recycling, which compensates for 47–64% of production impacts. In the GWP category, dominated by the battery cells and less the BOS components, the contribution of the transformer and the PCS is correspondingly smaller, but still significant. Noteworthily, the PCS, which includes the inverter, is excluded from the carbon footprint declaration under EU regulation, while the present work shows that adjusting the dimensioning of these components offers important potential for optimization.[49] In use cases with lower power requirements, such as load shifting over several hours, smaller transformers and power electronics could be used, substantially reducing the demand for high-impact materials. In contrast, a high-power use case would place greater demands on system cooling and require a more powerful TMS. Optimizing BOS components generally raises the question of balancing adequacy with efficiency. For instance, larger power electronics are typically more efficient than smaller ones. However, higher efficiencies are not required for every use case.[20] From an environmental impact perspective, BOS components should be precisely designed for each application to avoid excess size and impact.

When comparing the two cooling concepts, both offer distinct advantages. Liquid-cooling provides higher efficiency, with about 40% lower energy demand than air-cooling, and allows for a more compact system design.[96] Its higher thermal conductivity and specific heat capacity improve temperature control, leading to better overall system efficiency and reduced noise.[86] Air-cooling, on the other hand, offers a simpler and more cost-effective solution with no need for additional piping or cooling plates. It is easy to install and maintain, carries no leakage risk, and is well suited for systems with low heat generation, such as those operating at low C-rates.[86]

5. Limitations and future work

As in every LCA work, this study is subject to several limitations that further highlight promising directions for future work. First, the dimensioning of the system is based on a static approach, where all components are sized according to fixed design assumptions. A dynamic modeling framework, capable of adapting component sizes to the specific requirements of different use cases, would allow for a more flexible assessment and could provide valuable insights into system optimization. Building on the points raised in the discussion, it would be interesting investigate the trade-off between the efficiency and adequacy of BOS components in terms of environmental impact in a future study.

Second, the use phase modeling in this work is simplified through the application of an overall round-trip efficiency. While this provides a consistent basis for comparison, it does not capture the variability of operational conditions. A more detailed representation of use-phase losses, including real-time data on cooling demand, efficiency variations with the C-rate,

and the influence of cycle number and ambient conditions, would significantly increase the accuracy of the results. In particular, differences in climate and thermal management requirements associated with the operation and location of the system can have a major impact on the RTE. This is due to parasitic cooling or heating loads, as demonstrated by Olis *et al.* (2023).[97] Furthermore, future work should consider the electrochemical differences in battery cell ageing with regard to the cell type. This could allow optimization of the use of the batteries, *e.g.*, with regard to the depth of discharge.

Third, although this work is based on an extensive literature review incorporating more than 20 sources to provide one of the first full LCIs of a CSS, there remains a strong need for primary data, particularly regarding the detailed composition and manufacturing of system components. A similar limitation applies to the cell data, as primary data for SIBs in stationary applications are not yet available, necessitating the use of model-based literature inventories. In addition, the limitations of the underlying process data must be acknowledged. Although ecoinvent is the most widely used database in the literature, some of the processes it contains are outdated and should only be used when no other data is available. These processes should be critically examined and replaced with more recent data wherever possible.

Fourth, future research could also include a criticality assessment to complement the environmental analysis. Previous studies have shown notable differences in material criticality between SIBs and LIBs, typically favoring SIBs due to their use of more abundant and less geopolitically sensitive materials. Beyond environmental impacts, future assessments could be extended to cover economic and social dimensions of the life cycle, providing a more comprehensive evaluation of sustainability to inform decisions on the design and deployment of ESS.

Fifth, the specifications of the BOS components analyzed in this work may differ slightly depending on the system's energy, operation, use case, and location. It is assumed that there are no significant differences between the BOS components of CSS equipped with SIB and LIB, but to the best of the authors' knowledge, there is no publicly available information on the composition of a CSS with an SIB to support this assumption. The differences in discharge curves between SIBs and LIBs could be particularly important here because the more pronounced voltage drop of SIB during discharge might affect the operation of the power electronics.[98] Investigating the heat generation of the different battery types at various cycle rates at the system level would also be interesting in future studies.

6. Conclusions

This study is the first to establish a comprehensive LCI model for two different container storage systems (CSS), a liquid-cooled and an air-cooled system, including all balance of system (BOS) components. To ensure a realistic representation of the systems, great efforts were made to develop the LCI model based on the most prevalent design features and technologies currently available on the market. Taking a full life cycle approach, an in-depth assessment of the two systems with four different cell types was carried out, focusing on SIBs. The SIB technologies analyzed are based on three representative cathode active material (CAM) types: sodium manganese hexacyanoferrate (MnPBA) as a PBA, sodium vanadium fluorophosphate (NVPF) as a polyanionic material, and sodium nickel iron manganese oxide (NFM) as a layered metal oxide. Lithium iron phosphate (LFP)-based LIB serves as a reference. The identified key BOS components are the container, thermal management system (TMS), power conversion system (PCS), controller and auxiliary system. The PCS includes a bidirectional inverter and a transformer, which is usually housed in a separate cabinet outside the container. The auxiliary system comprises a fire suppression system, lighting, additional cabling, and the concrete foundation on which the system is placed.

The results show that BOS components contribute 32–58% of GWP impact and 63–88% of mineral resource use impact, emphasizing their significant role in the sustainability of grid-scale storage. The transformer's significant impact should be emphasized here, especially since it is explicitly excluded from the carbon footprint accounting under the EU regulation. This affects particularly the Mineral Resource Use category due to the large quantities of copper and steel contained in the transformer. However, its impact can be substantially reduced through adequate dimensioning and end of life recycling. Furthermore, the results show that under the considered framing conditions SIBs are competitive with LIBs in CSS with regard to environmental impacts, despite their lower energy densities. By shedding light on previously underexplored system elements, this work provides a robust foundation for more comprehensive LCAs of containerized storage solutions, enabling more informed design, scaling and policy decisions for future energy systems.

Author contributions

Friedrich B. Jasper: investigation, formal analysis, methodology, conceptualization, validation, writing – original draft, and visualization. Yuhuan Zhou: investigation, formal analysis, writing – original draft, and methodology. Hüseyin Ersoy: investigation, formal analysis, and validation. Manuel J. Baumann: conceptualization, supervision, writing – review & editing, validation, and project administration. Jens Peters: validation, writing – review & editing, and resources. Dirk Holger Neuhaus: validation, supervision, and project administration. Marcel Weil: conceptualization, supervision, writing – review & editing, validation, and project administration.

Conflicts of interest

There are no conflicts of interest to declare.

Data availability

The data supporting the findings of this study can be found in the supplementary information (SI) and at Zenodo under https://doi.org/10.5281/zenodo.17651912. Supplementary information is available. See DOI: https://doi.org/10.1039/d5ya00341e.

Acknowledgements

The authors acknowledge the financial support from the German Research Foundation (DFG) under Project ID 390874152 (POLiS Cluster of Excellence, EXC 2154). Furthermore, M.B. and M.W. acknowledge the basic funding from the Helmholtz Association, and J.P. acknowledges grant RYC2022-037773-I financed by the Ministry of Science and Innovation (MCIN/AEI/10.13039/501100011033) and by the ESF+. This work contributes to the research performed at CELEST (Center for Electrochemical Energy Storage Ulm-Karlsruhe).

References

1 T. Mahlia, T. Saktisahdan, A. Jannifar, M. Hasan and H. Matseelar, A review of available methods and development on energy storage; technology update, *Renewable Sustainable Energy Rev.*, 2014, **33**, 532–545.
2 M. A. Hannan, *et al.*, Battery energy-storage system: A review of technologies, optimization objectives, constraints, approaches, and outstanding issues, *J. Energy Storage*, 2021, **42**, 103023.
3 Y. Yang, Battery energy storage system size determination in renewable energy systems A review, *Renewable Sustainable Energy Rev.*, 2018, **91**, 109–125.
4 Y. Bu, Y. Wu, X. Li and Y. Pei, Operational risk analysis of a containerized lithium-ion battery energy storage system based on STPA and fuzzy evaluation, *Process Saf. Environ. Prot.*, 2023, **176**, 627–640.
5 S. Asiaban, *et al.*, Wind and Solar Intermittency and the Associated Integration Challenges: A Comprehensive Review Including the Status in the Belgian Power System, *Energies*, 2021, **14**, 2630.
6 Valuates reports. Global Container Type Battery Energy Storage Systems Market Research Report 2024. https://reports.valuates.com/market-reports/QYRE-Auto-20Q13585/global-container-type-battery-energy-storage-systems (2025).
7 Precedence research. Battery Energy Storage System Market Size, Share, and Trends 2024 to 2034. https://www.precedenceresearch.com/battery-energy-storage-system-market (2024).
8 ISO 14040. Environmental management - Life cycle assessment - Principles and framework, 2006.
9 ISO 14044. Environmental management – Life cycle assessment – Requirements and guidelines, 2006.
10 D. Paul, *et al.*, Life cycle assessment of lithium-based batteries: Review of sustainability dimensions, *Renewable Sustainable Energy Rev.*, 2024, **206**, 114860.
11 M. A. Pellow, H. Ambrose, D. Mulvaney, R. Betita and S. Shaw, Research gaps in environmental life cycle assessments of lithium ion batteries for grid-scale stationary energy storage systems: End-of-life options and other issues, *Sustainable Mater. Technol.*, 2020, **23**, e00120.
12 F. B. Jasper, *et al.*, Life cycle assessment (LCA) of a battery home storage system based on primary data, *J. Cleaner Prod.*, 2022, **366**, 132899.
13 M. Raugei, E. Leccisi and V. M. Fthenakis, What Are the Energy and Environmental Impacts of Adding Battery Storage to Photovoltaics? A Generalized Life Cycle Assessment, *Energy Technol.*, 2020, **8**, 1901146.
14 L. Da Silva Lima, *et al.*, Life cycle assessment of lithium-ion batteries and vanadium redox flow batteries-based renewable energy storage systems, *Sustain. Energy Technol. Assess*, 2021, **46**, 101286.
15 A. Abdon, *et al.*, Techno-economic and environmental assessment of stationary electricity storage technologies for different time scales, *Energy*, 2017, **139**, 1173–1187.
16 H. B. Komesse, M. Lucas, S. Duval—Dachary and S. Beauchet, A comprehensive cradle-to-grave life cycle assessment of three representative lithium-ion stationary batteries targeting a 20-year bi-daily charge–discharge service, *Int. J. Life Cycle Assess.*, 2024, **29**, 1246–1263.
17 S. Wickerts, R. Arvidsson, A. Nordelöf, M. Svanström and P. Johansson, Prospective Life Cycle Assessment of Lithium-Sulfur Batteries for Stationary Energy Storage, *ACS Sustainable Chem. Eng.*, 2023, **11**, 9553–9563.
18 C. Bauer, *Oekobilanz von Lithium-Ionen Batterien*, 2010.
19 G. Majeau-Bettez, T. R. Hawkins and A. H. Strømman, Life Cycle Environmental Assessment of Lithium-Ion and Nickel Metal Hydride Batteries for Plug-In Hybrid and Battery Electric Vehicles, *Environ. Sci. Technol.*, 2011, **45**, 4548–4554.
20 M. Schimpe, *et al.*, Energy efficiency evaluation of a stationary lithium-ion battery container storage system via electro-thermal modeling and detailed component analysis, *Appl. Energy*, 2018, **210**, 211–229.
21 P. Stanchev and N. Hinov, Comparative Techno-Economic and Life Cycle Assessment of Stationary Energy Storage Systems: Lithium-Ion, Lead-Acid, and Hydrogen, *Batteries*, 2025, **11**, 382.
22 Y. Li, *et al.*, Life cycle environmental hotspots analysis of typical electrochemical, mechanical and electrical energy storage technologies for different application scenarios: Case study in China, *J. Cleaner Prod.*, 2024, **466**, 142862.
23 X. Han, *et al.*, Comparative life cycle greenhouse gas emissions assessment of battery energy storage technologies for grid applications, *J. Cleaner Prod.*, 2023, **392**, 136251.
24 Y. Deng, J. Li, T. Li, X. Gao and C. Yuan, Life cycle assessment of lithium sulfur battery for electric vehicles, *J. Power Sources*, 2017, **343**, 284–295.
25 L. A. Ellingsen, *et al.*, Life cycle assessment of a lithium-ion battery vehicle pack, *J. Ind. Ecol.*, 2014, **18**, 113–124.
26 R. Yudhistira, D. Khatiwada and F. Sanchez, A comparative life cycle assessment of lithium-ion and lead-acid batteries for grid energy storage, *J. Cleaner Prod.*, 2022, **358**, 131999.
27 J. F. Peters and M. Weil, Providing a common base for life cycle assessments of Li-Ion batteries, *J. Cleaner Prod.*, 2018, **171**, 704–713.

28 C. Spanos, D. E. Turney and V. Fthenakis, Life-cycle analysis of flow-assisted nickel zinc-, manganese dioxide-, and valve-regulated lead-acid batteries designed for demand-charge reduction, *Renewable Sustainable Energy Rev.*, 2015, **43**, 478–494.
29 M. L. Carvalho, A. Temporelli and P. Girardi, Life Cycle Assessment of Stationary Storage Systems within the Italian Electric Network, *Energies*, 2021, **14**, 2047.
30 S. Weber, J. F. Peters, M. Baumann and M. Weil, Life cycle assessment of a vanadium redox flow battery, *Environ. Sci. Technol.*, 2018, **52**, 10864–10873.
31 D. A. Notter, *et al.*, Contribution of Li-ion batteries to the environmental impact of electric vehicles, 2010.
32 E. Leccisi, M. Raugei and V. Fthenakis, The energy and environmental performance of ground-mounted photovoltaic systems—a timely update, *Energies*, 2016, **9**, 622.
33 C. Jones, P. Gilbert and L. Stamford, Assessing the Climate Change Mitigation Potential of Stationary Energy Storage for Electricity Grid Services, *Environ. Sci. Technol.*, 2020, **54**, 67–75.
34 L. Vandepaer, J. Cloutier, C. Bauer and B. Amor, Integrating Batteries in the Future Swiss Electricity Supply System: A Consequential Environmental Assessment, *J. Ind. Ecol.*, 2019, **23**, 709–725.
35 L. Vandepaer, J. Cloutier and B. Amor, Environmental impacts of Lithium Metal Polymer and Lithium-ion stationary batteries, *Renewable Sustainable Energy Rev.*, 2017, **78**, 46–60.
36 L. A.-W. Ellingsen, C. R. Hung and A. H. Strømman, Identifying key assumptions and differences in life cycle assessment studies of lithium-ion traction batteries with focus on greenhouse gas emissions, *Transp. Res. D: Transp. Environ.*, 2017, **55**, 82–90.
37 N. A. Ryan, Y. Lin, N. Mitchell-Ward, J. L. Mathieu and J. X. Johnson, Use-Phase Drives Lithium-Ion Battery Life Cycle Environmental Impacts When Used for Frequency Regulation, *Environ. Sci. Technol.*, 2018, **52**, 10163–10174.
38 A. Burnham, M. Q. Wang and Y. Wu Development and Applications of GREET 2.7 – The Transportation Vehicle-CycleModel. ANL/ESD/06-5 https://www.osti.gov/servlets/purl/898530-scVqHc/(2006) , DOI: 10.2172/898530.
39 J. F. Peters and M. Weil, Aqueous hybrid ion batteries–An environmentally friendly alternative for stationary energy storage?, *J. Power Sources*, 2017, **364**, 258–265.
40 M. Zackrisson, L. Avellán and J. Orlenius, Life cycle assessment of lithium-ion batteries for plug-in hybrid electric vehicles – Critical issues, *J. Cleaner Prod.*, 2010, **18**, 1519–1529.
41 C. Bielitz Environmental and Economic Life-Cycle Assessment of Battery Technologies for Electricity Storage, 2016.
42 M. Baumann, J. F. Peters, M. Weil and A. Grunwald, CO2 Footprint and Life-Cycle Costs of Electrochemical Energy Storage for Stationary Grid Applications, *Energy Technol.*, 2017, **5**, 1071–1083.
43 D. A. Notter, *et al.*, Contribution of Li-ion batteries to the environmental impact of electric vehicles, 2010.
44 M. Hiremath, K. Derendorf and T. Vogt, Comparative Life Cycle Assessment of Battery Storage Systems for Stationary Applications, *Environ. Sci. Technol.*, 2015, **49**, 4825–4833.
45 International Energy Agency. Batteries and Secure Energy Transitions. https://www.iea.org/reports/batteries-and-secure-energy-transitions (2024).
46 Symtech Solar, Megatron 1.6 MW x 3 MWh BESS Datasheet, 2024.
47 EVESCO a Power-Sonic Corporation company, ES-10002000S Data sheet, 2022.
48 European Commission, Commission Recommendation (EU) 2021/2279, 2021.
49 European Parliament. Regulation (EU) 2023/1542 of the European Parliament and of the Council of 12 July 2023 Concerning Batteries and Waste Batteries, Amending Directive 2008/98/EC and Regulation (EU) 2019/1020 and Repealing Directive 2006/66/EC, 2023.
50 U. Datta, A. Kalam and J. Shi, A review of key functionalities of battery energy storage system in renewable energy integrated power systems, *Energy Storage*, 2021, **3**, e224.
51 M. A. Hannan, *et al.*, Battery energy-storage system: A review of technologies, optimization objectives, constraints, approaches, and outstanding issues, *J. Energy Storage*, 2021, **42**, 103023.
52 S. Andreasi Bassi, *et al.*, Rules for the Calculation of the Carbon Footprint of Industrial Batteries without External Storage (CFB-IND), (Publications Office of the European Union, 2025).
53 M. Shen and Q. Gao, A review on battery management system from the modeling efforts to its multiapplication and integration, *Int. J. Energy Res.*, 2019, **43**, 5042–5075.
54 C. Hang, P. Liu, M. An, X. Chen and B. Chen, MW-Class Containerized Energy Storage System Scheme Design and Engineering Application. in 2023 2nd Asia Power and Electrical Technology Conference (APET) 801–805 (IEEE, Shanghai, China, 2023), DOI: 10.1109/APET59977.2023.10489583.
55 Y. Bu, Y. Wu, X. Li and Y. Pei, Operational risk analysis of a containerized lithium-ion battery energy storage system based on STPA and fuzzy evaluation, *Process Saf. Environ. Prot.*, 2023, **176**, 627–640.
56 Y. Guo, *et al.*, Modeling and analysis of liquid-cooling thermal management of an in-house developed 100 kW/500 kWh energy storage container consisting of lithium-ion batteries retired from electric vehicles, *Appl. Therm. Eng.*, 2023, **232**, 121111.
57 Y. Ding, W. Chu and Q. Wang, Airflow reorganization and thermal management in a large-space battery energy storage container using perforated deflectors, *Int. Commun. Heat Mass Transfer*, 2024, **158**, 107909.
58 M. Akbarzadeh, *et al.*, A comparative study between air cooling and liquid cooling thermal management systems for a high-energy lithium-ion battery module, *Appl. Therm. Eng.*, 2021, **198**, 117503.
59 S. Zhang, F. Nie, J. Cheng, H. Yang and Q. Gao, Optimizing the air flow pattern to improve the performance of the air-cooling lithium-ion battery pack, *Appl. Therm. Eng.*, 2024, **236**, 121486.

60 M. Chen, B. Zhang, Y. Li, G. Qi and J. Liu, Design of a multi-level battery management system for a Cascade H-bridge energy storage system. in 2014 IEEE PES Asia-Pacific Power and Energy Engineering Conference (APPEEC) 1–5 (IEEE, Hong Kong, 2014), DOI: 10.1109/APPEEC.2014.7066076.
61 P. Voß, *et al.*, Benchmarking state-of-the-art sodium-ion battery cells – modeling energy density and carbon footprint at the gigafactory-scale, *Energy Environ. Sci.*, 2025, **18**, 8104.
62 F. B. Jasper, *et al.*, Comparative Life Cycle Assessment of Prussian White and NVP/C-Based Sodium-Ion Batteries Based on Primary Laboratory Data, *ChemSusChem*, 2025, 2500268.
63 Y. Gao, *et al.*, A 30-year overview of sodium-ion batteries, *Carbon Energy*, 2024, **6**, e464.
64 S. Hasselwander, M. Meyer and I. Österle, Techno-Economic Analysis of Different Battery Cell Chemistries for the Passenger Vehicle Market, *Batteries*, 2023, **9**, 379.
65 NOVONIX, Sodium-Ion Batteries at NOVONIX: Market Landscape, Materials Overview, and Industry R&D Trends, https://www.novonixgroup.com/news/sodium-ion-batteries-at-novonix-market-landscape-materials-overview-and-industry-rd-trends/(2025).
66 T. Carrère, U. Khalid, M. Baumann, M. Bouzidi and B. Allard, Carbon footprint assessment of manufacturing of synthetic graphite battery anode material for electric mobility applications, *J. Energy Storage*, 2024, **94**, 112356.
67 F. Degen, M. Winter, D. Bendig and J. Tübke, Energy consumption of current and future production of lithium-ion and post lithium-ion battery cells, *Nat. Energy*, 2023, **8**, 1284–1295.
68 M. Baumann, J. Peters and M. Weil, Exploratory Multi-criteria Decision Analysis of Utility-Scale Battery Storage Technologies for Multiple Grid Services Based on Life-Cycle Approaches, *Energy Technol.*, 2020, **8**, 1901019.
69 M. McKinnon, A. Barowy, A. Schraiber and J. Regan, Full-scale walk-in containerized lithium-ion battery energy storage system fire test data, *Data in Brief*, 2022, **45**, 108712.
70 Midea Group, Environmental Product Decleration for Split-type Room Air Conditioner (S-P-06897), 2023.
71 Hua Power, 500kW/1MWh LFP Battery Energy Storage System with Air-Cooling. Zhejiang Hua Power Co.,Ltd, https://www.ihuapower.com/sale-38865884-lfp-battery-500kw-1075kwh-1mwh-air-conditioning-cooling-integrated-energy-storage-system-with-custom.html, 2025.
72 Y. Xian, *et al.*, Study on uniform distribution of liquid cooling pipeline in container battery energy storage system, *J. Energy Storage*, 2025, **112**, 115395.
73 P. Catrini, M. Cellura, F. Guarino, D. Panno and A. Piacentino, An integrated approach based on Life Cycle Assessment and Thermoeconomics: Application to a water-cooled chiller for an air conditioning plant, *Energy*, 2018, **160**, 72–86.
74 LNEYA, Energy Storage Liquid Cooling Constant Temperature Unit CNYL-45.
75 C. Hunziker, J. Lehmann, T. Keller, T. Heim and N. Schulz, Sustainability assessment of novel transformer technologies in distribution grid applications, *Sustain. Energy Grids Netw.*, 2020, **21**, 100314.
76 Daelim, 1200 kVA Substation Transformer-13.8kV, https://www.daelimtransformer.com/1200-kva-substation-transformer.html.
77 Larson Electronics, 1800 kVA Distribution Transformer - 480V Delta Primary - 220Y/127 Wye-N Secondary - NEMA 3R - 60Hz, https://www.larsonelectronics.com/product/295468/1800-kva-distribution-transformer-480v-delta-primary-220y-127-wye-n-secondary-nema-3r-60hz?srsltid=AfmBOorC28F0l-Xp8yz7ea2zRgXLdPj1FTN0GyKGCHiyyn83B8Btw1Y_&utm_source=chatgpt.com.
78 Lazard Inc. Levelized Cost of Energy+, 2024.
79 IEA, Renewables 2024 – Analysis and Forecasts to 2030, https://www.iea.org/reports/renewables-2024, 2024.
80 A. Parlikar, H. Hesse and A. Jossen, Topology and Efficiency Analysis of Utility-Scale Battery Energy Storage Systems, in 119–131 (Atlantis Press, 2019).
81 DEA - Danish Energy Agency. Energy Storage - Technology Descriptions and Projections for Long-Term Energy System Planning, 2018.
82 IRENA, Battery storage and renewables: costs and markets to 2030, International Renewable Energy Agency, https://www.irena.org/Publications/2017/Oct/Electricity-storage-and-renewables-costs-and-markets, 2017.
83 D. Keiner, *et al.*, Sodium-ion battery cost projections and their impact on the global energy system transition until 2050, *J. Energy Storage*, 2026, **146**, 119861.
84 J. F. Peters, M. Baumann, J. R. Binder and M. Weil, On the environmental competitiveness of sodium-ion batteries under a full life cycle perspective – a cell-chemistry specific modelling approach, *Sustainable Energy Fuels*, 2021, **5**, 6414–6429.
85 J. Peters, D. Buchholz, S. Passerini and M. Weil, Life cycle assessment of sodium-ion batteries, *Energy Environ. Sci.*, 2016, **9**, 1744–1751.
86 K. S. Garud, L. D. Tai, S.-G. Hwang, N.-H. Nguyen and M.-Y. Lee, A Review of Advanced Cooling Strategies for Battery Thermal Management Systems in Electric Vehicles, *Symmetry*, 2023, **15**, 1322.
87 H. A. A. Ali and Z. N. Abdeljawad, Thermal Management Technologies of Lithium-Ion Batteries applied for Stationary Energy Storage Systems, 2020.
88 M. Xue, A. Kendall, Z. Xu and J. M. Schoenung, Waste Management of Printed Wiring Boards: A Life Cycle Assessment of the Metals Recycling Chain from Liberation through Refining, *Environ. Sci. Technol.*, 2015, **49**, 940–947.
89 E. Olsson, Screening Life Cycle of Recycled Glycol, https://www.glykoli.fi/wp-content/uploads/2025/01/recyctec-official-report-nov-2018.pdf?utm_source=chatgpt.com, 2018.
90 J. Litardo, *et al.*, Air-conditioning life cycle assessment research: A review of the methodology, environmental impacts, and areas of future improvement, *Energy Build.*, 2023, **296**, 113415.
91 Larsson, M. C. Ageing of Industrial Control Systems (ICS).

92 EPRI, Distributed Control System Life Cycle Management: Guidelines for Planning and Managing the Life Cycle of Distributed Control Systems, 2013.
93 W. J. Hassel, Liquid versus Air: Life Cycle Carbon of Cooling Down AI Data Centers, Master's thesis, Harvard University Division of Continuing Education, Harvard, 2025.
94 C. Bucher, J. Wandel and D. Joss, Life expectancy of pv inverters and optimizers in residential pv systems, WCPEC-8: EU PVSEC Proceedings, https://www.bfh.ch/dam/jcr:5bfd5c32-f70f-4bf6-8d60-fdab6094e164/2022_09_WCPEC-8_3DV.1.46_-_Life_Expectancy_of_PV_inverters.pdf, 2022.
95 S. Zhang, B. Steubing, H. Karlsson Potter, P.-A. Hansson and Å. Nordberg, Future climate impacts of sodium-ion batteries, *Resour., Conserv. Recycl.*, 2024, **202**, 107362.
96 C. Wu, *et al.*, A review on the liquid cooling thermal management system of lithium-ion batteries, *Appl. Energy*, 2024, **375**, 124173.
97 W. Olis, D. Rosewater, T. Nguyen and R. H. Byrne, Impact of heating and cooling loads on battery energy storage system sizing in extreme cold climates, *Energy*, 2023, **278**, 127878.
98 M. Rehm, *et al.*, Comparing the electrical performance of commercial sodium-ion and lithium-iron-phosphate batteries, *J. Power Sources*, 2025, **633**, 236290.